

# On the Viability of Tadalafil-Based $^{18}\text{F}$ -Radiotracers for *In Vivo* Phosphodiesterase 5 (PDE5) PET Imaging

Justin J. Bailey,\* Melinda Wuest, Tamara Bojovic, Travis Kronemann, Carmen Wängler, Björn Wängler, Frank Wuest, and Ralf Schirmmacher



Cite This: *ACS Omega* 2021, 6, 21741–21754



Read Online

ACCESS |



Metrics & More

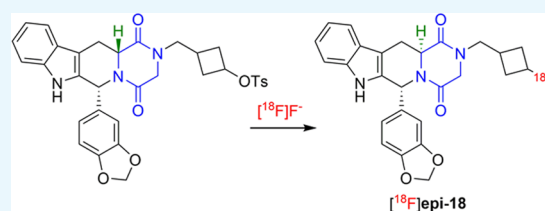


Article Recommendations



Supporting Information

**ABSTRACT:** Phosphodiesterase 5 (PDE5) is a clinically relevant biomarker and therapeutic target for many human pathologies, yet a noninvasive agent for the assessment of PDE5 expression has yet to be realized. Such agents would improve our understanding of the nitric oxide (NO)/cyclic guanosine 3',5'-monophosphate (cGMP)/PDE5 pathway in human pathologies and potentially lead to novel uses of PDE5 inhibitors to manage lung conditions like SARS-CoV-2-mediated pulmonary inflammatory responses. In this study, efforts were made to produce an  $^{18}\text{F}$ -labeled analogue of the PDE5 inhibitor tadalafil to visualize PDE5 expression *in vivo* with positron emission tomography (PET). However, during the late-stage fluorination step, quantitative epimerization of the tadalafil C12a stereocenter occurred, yielding a less active epi-isomer. *In vivo* dynamic microPET images in mice revealed that the epimerized radiotracer, [ $^{18}\text{F}$ ]epi-18, rapidly accumulated in the liver with negligible uptake in tissues of known PDE5 expression.



## INTRODUCTION

Cyclic nucleotide phosphodiesterases (PDEs) are a superfamily of metallophosphohydrolases, which metabolically inactivate the secondary messenger molecules, cyclic adenosine 3',5'-monophosphate (cAMP), and cyclic guanosine 3',5'-monophosphate (cGMP), by cleavage of their phosphodiester bond. These secondary messengers are important regulators of intracellular signal transduction, translating extracellular responses from primary signaling molecules such as hormones, neurotransmitters, or cytokines into a cellular response. Under normal physiological conditions, cyclic nucleotides mediate numerous cellular homeostatic processes, such as cell proliferation, reproduction, immune/inflammatory responses, neuronal signaling, and muscle relaxation. Consequently, dysregulated cyclic nucleotide signaling is implicated in initiating and modulating pathophysiological processes responsible for many clinically relevant disease states, including Alzheimer's disease (AD), schizophrenia, arthritis, chronic obstructive pulmonary disease, pulmonary hypertension, erectile dysfunction (ED), and cancer.<sup>1,2</sup> As PDEs provide a mechanism for controlling the amplitude, duration, and termination of cyclic nucleotide-dependent signaling, they have been exploited by a number of pharmacological agents as a prognostic indicator and therapeutic target.<sup>3,4</sup>

Of the 11 distinct isozymes (PDE1–PDE11) in the PDE superfamily, phosphodiesterase 5 (PDE5) has garnered considerable attention following the serendipitous discovery of PDE5 as a therapeutic target for treating ED. Sildenafil, the prototypical inhibitor of PDE5 (Figure 1), was originally developed by Pfizer in 1989 for the treatment of hypertension

and angina pectoris.<sup>5</sup> While early clinical trials indicated marginal benefits in treating coronary artery disease, male participants reported an interesting erectogenic “adverse effect” from the drug arising from off-tissue PDE5 inhibition in the corpus cavernosum smooth muscle in the penis.<sup>6</sup> Sildenafil citrate (Viagra, Pfizer) was subsequently approved a decade later by the Food and Drug Administration (FDA) for the treatment of ED. Academic and preclinical/clinical industrial drug discovery programs have since sought out more potent and selective PDE5 inhibitors, leading to the approval of three additional PDE5 inhibitors for ED management: tadalafil (Cialis, Eli Lilly) and vardenafil (Levitra, Bayer/GlaxoSmithKline) in 2003, and avanafil (Stendra, Vivus) in 2012. Sildenafil and tadalafil have since been approved to treat pulmonary arterial hypertension, branded as Revatio and Adcirca, respectively,<sup>7</sup> and tadalafil to treat benign prostatic hyperplasia.<sup>8</sup>

Expression of PDE5 is not limited to the corpus cavernosum and cardiovascular tissues and is present in virtually all human cell types, tissues, and organs.<sup>3,9</sup> There has thus been a strong interest over the past two decades to explore new clinical applications for PDE5 inhibitors and consider new mechanisms of action outside of their known vasodilatory effects.

Received: June 24, 2021

Accepted: July 29, 2021

Published: August 12, 2021



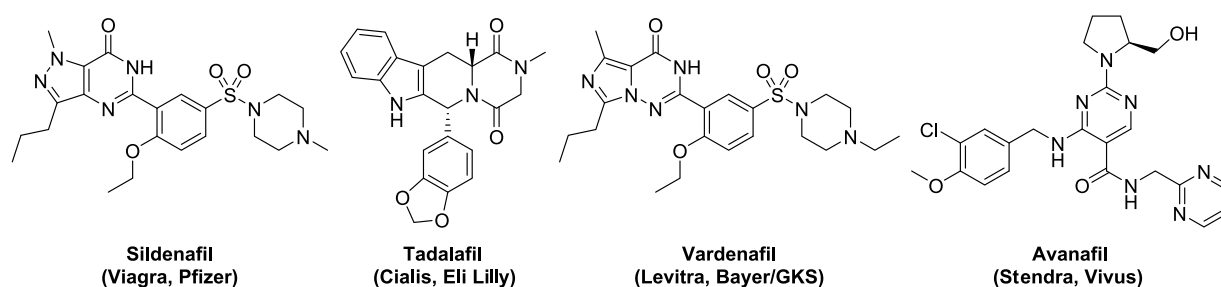


Figure 1. FDA-approved PDE5 inhibitors.

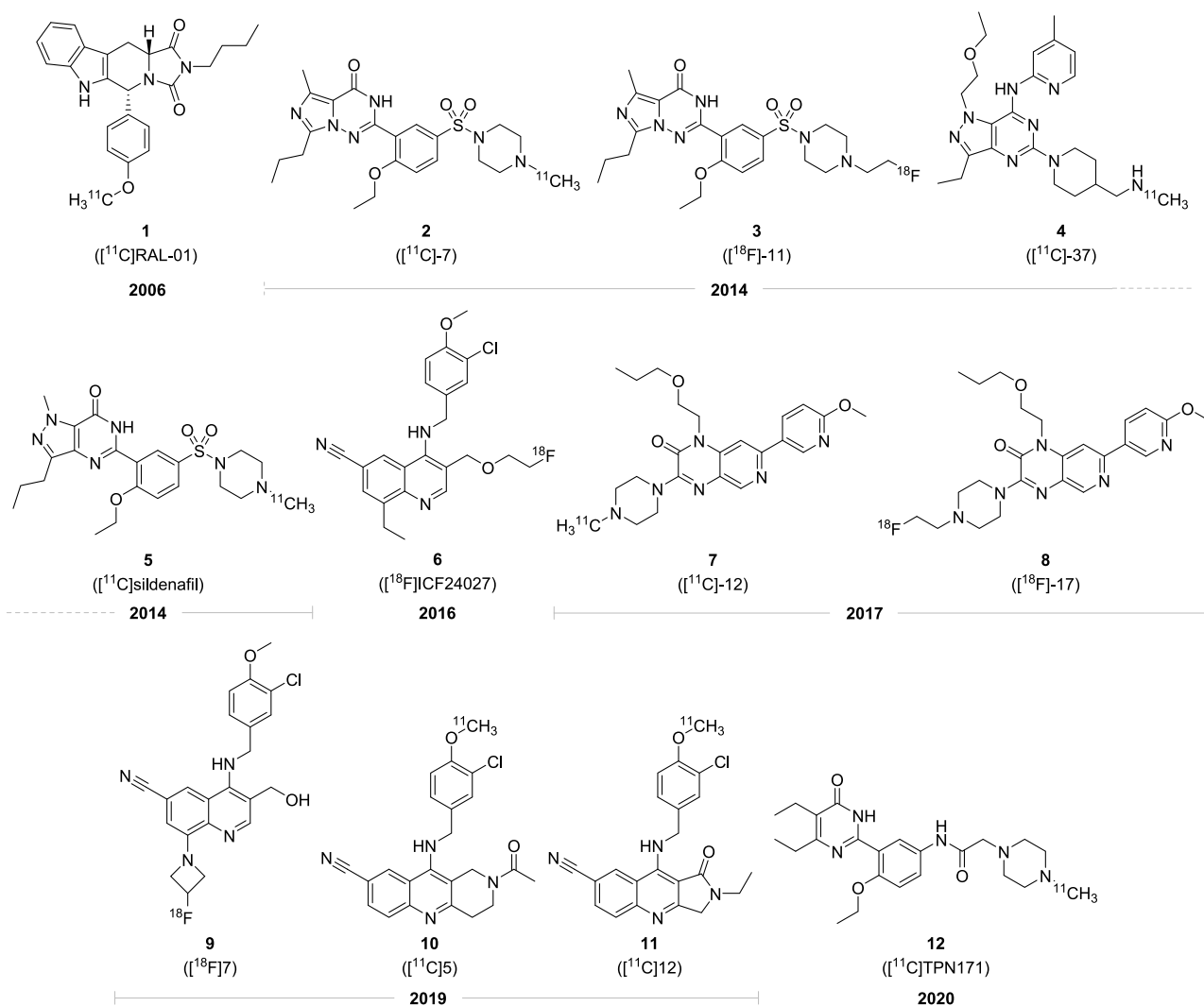
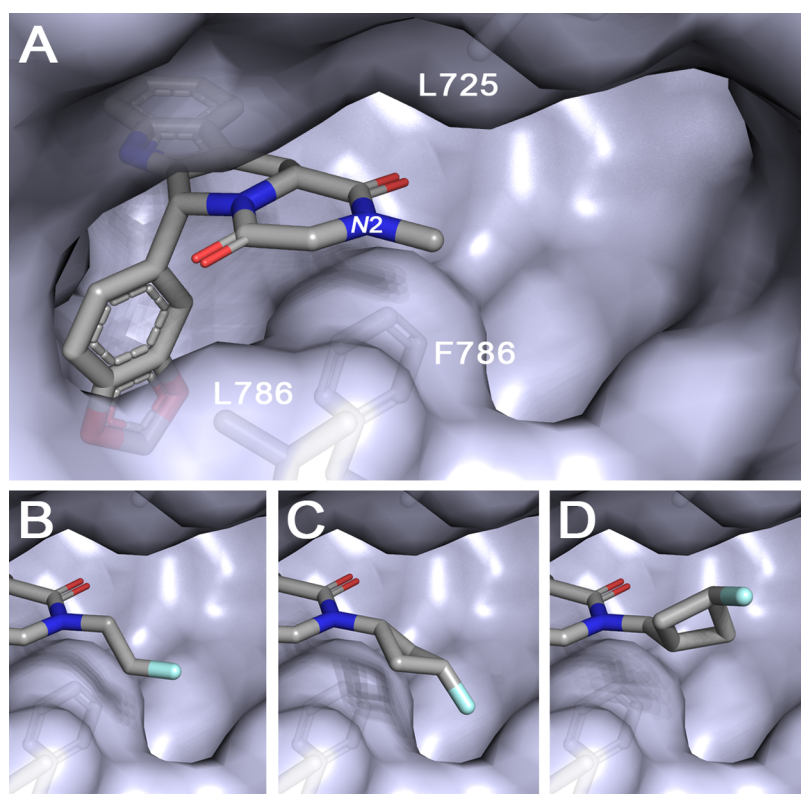


Figure 2. Previous radiotracers designed for imaging PDE5 with PET over the last two decades. The compound labels from the originating publications are denoted in brackets.

Numerous clinical and preclinical studies are underway investigating the use of approved and experimental PDE5 inhibitors in managing genitourinary dysfunctions such as benign prostatic hyperplasia, premature ejaculation, urinary tract calculi, overactive bladder, Peyronie's disease, and priapism.<sup>10</sup> A growing number of human cancers have also been found to overexpress PDE5,<sup>11–13</sup> instigating the clinical exploration of PDE5 inhibitors as chemosensitizers.<sup>14</sup> In the brain, PDE5 has been targeted to treat neurodegeneration, neuroinflammation, and cognitive dysfunction due to the connection of the nitric oxide (NO)/cGMP/pCREB pathway

to these disease states.<sup>15</sup> Most recently, the use of PDE5 inhibitors has been proposed to counter thromboembolic episodes caused by the inflammatory cascade in COVID-19 patients,<sup>16</sup> given the high level of expression of PDE5 in the lungs and the involvement of the NO/cGMP pathway in COVID-19 inflammatory processes.<sup>17</sup> There are currently three clinical trials underway investigating the therapeutic efficacy of sildenafil with COVID-19 patients.<sup>18</sup>

The selected findings described herein highlight the importance of PDE5 modulation and its potential as a prognostic and therapeutic target. Yet there exists no approved



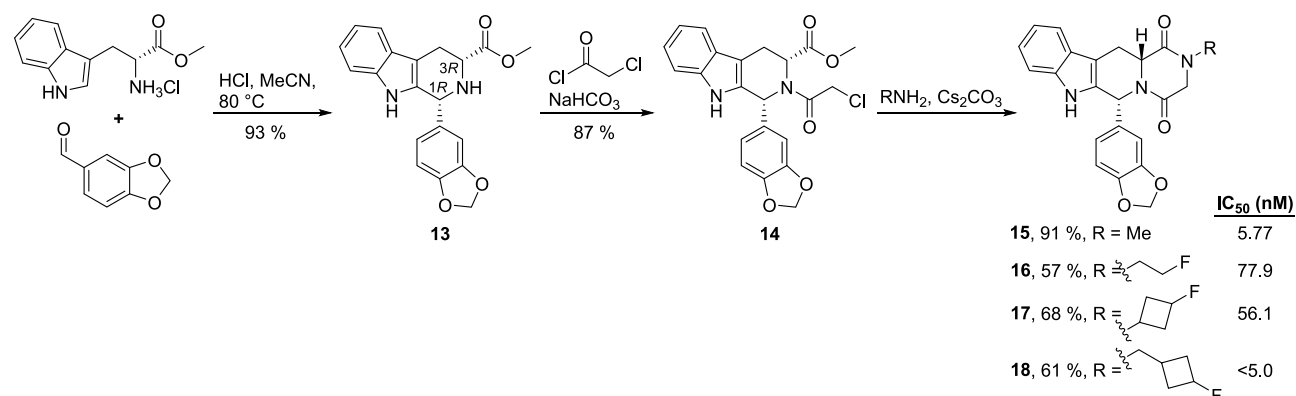
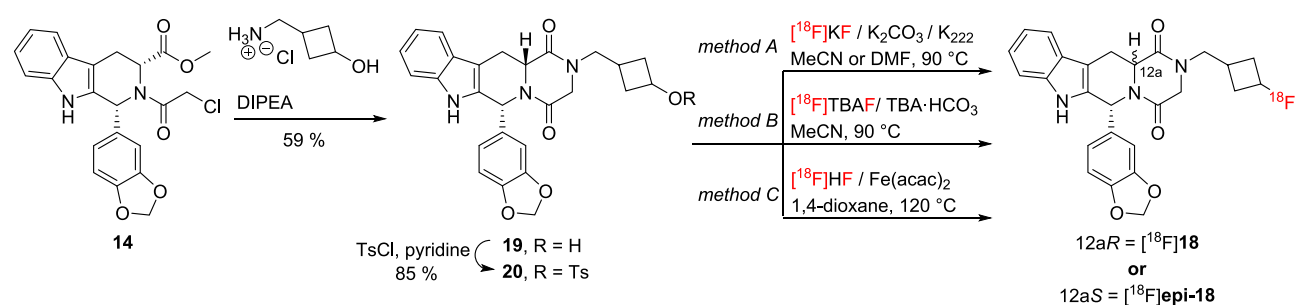
**Figure 3.** Tadalafil and its N2-substituted analogues in the binding pocket of PDE5. (A) Cocrystal structure of tadalafil **5**, with PDE5 (PDB: 1XOZ). (B) *N*-Fluoroethyl **16**, (C) *N*-fluorocyclobutyl **17**, and (D) *N*-(fluorocyclobutyl)methyl **18** analogues of tadalafil docked in PDE5.

method to noninvasively evaluate the level of PDE5 expression *in vivo* to better elucidate its role in normal and pathological conditions. Positron emission tomography (PET) is a sensitive and minimally invasive imaging technique that allows for the three-dimensional (3D) mapping of molecular targets in a biological system using radiotracers labeled with short-lived positron-emitting radionuclides. Radiotracers specific for PDE5 would offer the ability to quantify and evaluate spatiotemporal changes of PDE5 expression in various disease states, reveal the systemic pharmacokinetics and biodistribution of the nonradioactive parent compound for dose regimen optimization, and identify patients that would benefit from treatments utilizing PDE5 inhibitors.

The first radiotracers explored for PDE5 imaging with PET were the  $^{11}\text{C}$ - and  $^{18}\text{F}$ -labeled derivatives of tadalafil, sildenafil, and vardenafil (compounds **1–5**, Figure 2). These early tracers displayed varying degrees of PDE5-specific binding in the myocardium and pulmonary tissue in animal models, tissues of known PDE5 expression, but no specific uptake in the brain or other tissues.<sup>19–21</sup> Rapid plasma metabolism, radiometabolite accumulation, and extensive serum albumin binding were reported in cases where radiotracer metabolism was investigated. As quantitative PET studies of PDE5 in the brain are of considerable interest for studying disease, efforts have since shifted toward radiolabeling novel brain penetrant PDE5 inhibitors of improved potency to overcome the suspected low receptor density in the brain ( $B_{\text{max}} \approx 0.1 \text{ nM}$ ).<sup>22</sup> The  $^{18}\text{F}$ -labeled quinoline **6** was developed specifically as a brain imaging agent based on its high PDE5 potency ( $\text{IC}_{50} = 1.86 \text{ nM}$ ), selectivity over PDE6 and PDE11, and its potential to cross the blood–brain barrier (BBB).<sup>23,24</sup> Despite its potential, high nonspecific binding was observed in the brain due to the

rapid formation of a brain penetrable radiometabolite arising from O- $^{18}\text{F}$ -dealkylation. A 3- $^{18}\text{F}$ fluoroazetidine ring was later substituted in place of the ethyl group on the quinoline ring (compound **9**, Figure 2) in an effort to increase metabolic stability, but were ineffective.<sup>25</sup> Similar results were reported for the  $^{11}\text{C}$ - and  $^{18}\text{F}$ -labeled pyridopyrazinones **7** and **8**, *i.e.*, PDE5-nonspecific brain retention and extensive O- and N-dealkylation metabolic degradation.<sup>26</sup> The low specific brain uptake of these radiotracers may be attributed to too low of an affinity for PDE5 for *in vivo* visualization at the natural levels of expression of PDE5. The latest PDE5-targeting radiotracers, quinolines **10** and **11**, and 4(3*H*)-pyrimidinone **12**, have been developed as high-potency PET tracers ( $\text{IC}_{50} = 0.056, 0.059, 0.62 \text{ nM}$ , respectively) for imaging PDE5 in AD and heart disease, although their use in animal or tissue studies has yet to be reported.<sup>27,28</sup>

Despite these efforts, no radiotracer developed for PDE5 imaging has successfully been described. To further our understanding of PDE5 expression in normal and pathological states, a series of novel fluorinated tadalafil analogues were synthesized to identify a lead structure suitable for translation into an  $^{18}\text{F}$ -labeled radiotracer. While tadalafil does not have the necessary affinity ( $K_d = 2.9 \pm 3.8 \text{ nM}$ ) to achieve a threshold binding potential suitable for baseline PDE5 imaging in the brain (estimated  $B_{\text{max}}$  of  $0.1 \text{ nM}$ ),<sup>22</sup> a tadalafil-based radiotracer may prove useful to study brain pathologies where PDE5 is significantly overexpressed (AD patients exhibit a >5-fold increase in PDE5 brain expression),<sup>29</sup> or in tissues where PDE5 expression is innately high, such as in the lungs ( $B_{\text{max}}$  of >200 nM in rats).<sup>30</sup> In the latter case, such a tracer would prove useful in elucidating the prospective role of PDE5 in pulmonary inflammation caused by SARS-CoV-2 infection,

Scheme 1. Synthesis of Fluorinated Tadalafil Analogues and Their Respective IC<sub>50</sub> ValuesScheme 2. Synthesis of Precursor 20 for Radiolabeling, and <sup>18</sup>F-Radiolabeling Conditions Evaluated for Tosylate Displacement with [<sup>18</sup>F]Fluoride

and the therapeutic value of PDE5 inhibitors in the management of COVID-19.

## RESULTS AND DISCUSSION

The *N*-methyl group of tadalafil was chosen for structural modification to accommodate <sup>18</sup>F-incorporation based on the synthetic accessibility and the documented acceptance of structurally diverse functionalities at this position. Tadalafil, and *N*2-substituted analogues thereof, are predominantly synthesized through a three-step process wherein methylamine, or an analogue amine, is used to propagate the cyclization of the 2,5-diketopiperazine ring in the terminal step of the synthesis (*vide infra*). The *N*2-nitrogen is also orientated toward a large solvent exposed pocket within the PDE5 active site (Figure 3A), accounting for the acceptance of substituents at this position.<sup>31,32</sup> Three fluorinated tadalafil analogues were synthesized to identify a suitable lead with retained PDE5 affinity for later translation into an <sup>18</sup>F-isotopologue for PET. Analogues bearing the *N*2-fluoroethyl, *N*2-fluorocyclobutyl, and *N*2-(fluorocyclobutyl)methyl were chosen due to their small size, which would minimally impact the pharmacokinetics from that of the parent structure. Unexpectedly, molecular docking of these analogues in the active site of PDE5 revealed similar binding modes to tadalafil, with the *N*2 substitutions well tolerated (Figure 3B–D).

While it was anticipated that the creation of an *N*2-[<sup>18</sup>F]fluoroethyl tadalafil analogue through direct fluorination means could be problematic due to the formation of competing oxazoline and oxazolidine byproducts, the *N*2-fluoroethyl analogue was still included in the study to facilitate a direct comparison of its binding affinity against the larger fluorocyclopropyl analogues. Utilizing the fluorocyclobutyl rings reduces the flexibility of the pendant *N*2-group and

discourages the intramolecular cyclization needed for the oxazoline formation. Additionally, while [<sup>18</sup>F]fluoroalkyl chains are prone to *O*- and *N*-defluoroalkylation *in vivo* through cytochrome P450 monooxygenases metabolism, replacement with an [<sup>18</sup>F]fluorocycloalkyl ring can result in greater metabolic stability.<sup>33</sup> This strategy has been successfully employed in the creation of the metabolically stable leucine and tyrosine analogues 1-amino-3-[<sup>18</sup>F]fluorocyclobutane-1-carboxylic acid ([<sup>18</sup>F]FACBC) and 3-[<sup>18</sup>F]fluorocyclobutyl-L-tyrosine (L-3-[<sup>18</sup>F]FCBT).<sup>34,35</sup>

The key *N*-chloroacetyl tetrahydro- $\beta$ -carboline intermediate **14** was synthesized according to the standard procedure, beginning with the Pictet–Spengler reaction of *D*-tryptophan methyl ester hydrochloride with piperone to yield the tetrahydro- $\beta$ -carboline **13** (Scheme 1).<sup>36,37</sup> The (1*R*,3*R*)-diastereoisomer of **13** can be near exclusively formed through the crystallization-induced asymmetric transformation (CIAT) process. (1*R*,3*R*)-Carboline **13** was then acylated to provide *N*-chloroacetyl **14**, which then underwent nucleophilic displacement with a selection of alkyl amines, followed by cyclization to form the final 2,5-diketopiperazines **15–18**.

The PDE5 inhibitory activities of tadalafil, **15**, and the fluorinated analogues **16–18** were evaluated using the Transcreener AMP<sup>2</sup>/GMP<sup>2</sup> platform to elucidate the potential impact of the *N*2-substitutions on target binding. As IC<sub>50</sub> values are dependent on the conditions used in any given assay, tadalafil **15** was included as a reference compound. The *N*2-fluoroethyl **16**, *N*2-fluorocyclobutyl **17**, and *N*2-(fluorocyclobutyl)methyl **18** analogues displayed a PDE5 IC<sub>50</sub> values of 77.9, 56.1, and <5.0 nM, respectively, in comparison to 5.77 nM for tadalafil **15**. Curiously, the least sterically bulky *N*2-fluoroethyl analogue **16** exhibited the greatest affinity loss, while *N*2-(fluorocyclobutyl)methyl

analogue **18** had comparable potency to tadalafil **15**. The N2-fluorocyclobutyl **17** analogue displayed over 10-fold decreased potency compared to tadalafil **15**, which may be a result of steric clash with the L725, F786, and L804 side chains flanking the periphery to the active site (Figure 3A). These results confirm that the fluorinated N2-substitutions requisite for  $^{18}\text{F}$ -radiolabeling are tolerated well and minimally affect the binding affinity to PDE5. Analogue **18** was selected for translation into an  $^{18}\text{F}$ -labeled tracer for PDE5 imaging *via* PET due to its comparable binding affinity to that of parent tadalafil.

A methylbenzenesulfonate (tosylate) precursor **20** was prepared as shown in Scheme 2, which provides a suitable leaving group for radiolabeling *via* aliphatic nucleophilic substitution with  $^{18}\text{F}$ fluoride. The amination and cyclization of *N*-chloroacetyl **14** with 3-(aminomethyl)cyclobutanol hydrochloride proceeded smoothly to obtain alcohol **19**, which was then treated with tosyl chloride to create precursor **20**.

The radiolabeling of precursor **20** with  $^{18}\text{F}$ fluoride was first investigated using the conventional potassium carbonate ( $\text{K}_2\text{CO}_3$ ) and Kryptofix 222 ( $\text{K}_{222}$ ) labeling complex ( $^{18}\text{F}\text{KF}/\text{K}_2\text{CO}_3/\text{K}_{222}$ ), as shown in Scheme 2, method A. In brief, an  $^{18}\text{F}$ fluoride stock solution is prepared by eluting trapped  $^{18}\text{F}$ fluoride from an anion exchange cartridge with a solution of  $\text{K}_2\text{CO}_3 \cdot \text{K}_{222}$ , which is then azeotropically dried and reconstituted with 1 mL of  $\text{CH}_3\text{CN}$  or dimethylformamide (DMF). The labeling of precursor **20** (1 mg, 1.6  $\mu\text{mol}$ ) was performed at 90 °C using a 200  $\mu\text{L}$  aliquot of the resulting  $^{18}\text{F}\text{KF}/\text{K}_2\text{CO}_3/\text{K}_{222}$  stock solution, equaling  $\sim 200$  MBq  $^{18}\text{F}$ fluoride. The radiochemical conversion (RCC) of precursor **20** was determined after 10 or 20 min reaction time by radio-high-performance liquid chromatography (radio-HPLC) analysis of an aliquot of the reaction solution, calculated as the fraction of non-decay-corrected (n.d.c.) radioactivity of the isolated product from the total radioactivity of the sample injected (Table 1, entries 1–4). On first observation, the reaction proceeded cleanly in  $\text{CH}_3\text{CN}$ , yielding a single-labeled product and only one major byproduct which elutes just after precursor **20** (Figure 4A). An RCC of  $\sim 7\%$  was achieved after 10 min, which doubled to  $\sim 15\%$  after 20 min, with an apparent molar activity ( $A_m$ ) of

56–89 GBq/ $\mu\text{mol}$  ( $n = 3$ , end of synthesis (EOS)). The labeling reaction did not proceed when the reaction temperature was reduced to 60 °C, or when performed in DMF (Table 1, entries 3–5). During the quality control (QC) HPLC analysis of these initial reactions with co-injected standard **18**, it was discovered that the 12.42 min retention time of the radio-peak was suspiciously delayed from what was expected to correspond with the 11.63 UV absorbance peak from standard **18** (Figure 4B). In our laboratory setup, there is normally a 10–15 s delay between when the UV and radioactivity signals are registered from a radiolabeled compound due to the length tubing between the UV and radioactivity detectors in our HPLC system. In the case of the isolated radiolabeled product, the radio-peak eluted approximately 47 s after standard **18**, indicating that the radiotracer was not  $^{18}\text{F}$ **18**.

It has been reported in the literature that tadalafil can undergo a base-catalyzed epimerization at the C12a position to form a thermodynamically stable (6*R*,12*aS*)-stereoisomer, as the proton adjacent to the carbonyl at the C1 position is mildly acidic (Scheme 3).<sup>32,38</sup> This epimerization may occur during the radiolabeling of precursor **20** due to the basic conditions at elevated temperatures, which could be detrimental for PDE5 imaging as the absolute configuration of tadalafil is of vital importance for substrate recognition.<sup>32</sup> To test this hypothesis and determine the effect of  $^{18}\text{F}$ **18** epimerization on PDE5 binding potency, C12a epimers of compounds **15** and **18** were synthesized (Scheme 3). Quantitative epimerization to the (6*R*,12*aS*)-stereoisomers was easily achieved by refluxing the (6*R*,12*aR*)-isomers in a solution of 5:1 DMF/ $\text{K}_2\text{CO}_3$  (sat. aq) for 10 min. Evaluation of the PDE5 inhibitory activities of *epi-15* and *epi-18* revealed a 100-fold decrease in binding potency (Scheme 3). Such a loss in activity is consistent with other (6*R*,12*aS*)-stereoisomers of tadalafil analogues in the literature.<sup>39,40</sup> When injected onto HPLC, the UV peak of *epi-18* emerged 10 s ahead of the primary radio-peak from the radiosynthesis (Figure 5), matching the expected time delay between our detectors and verifying that the isolated product is most likely  $^{18}\text{F}$ *epi-18*. These findings also suggest that the major byproduct formed during the radiolabeling reaction and eluted  $\sim 45$  s after precursor **20** is the epimer of **20** (Figure 4A and Figure S1, Supporting Information).

To avoid the epimerization of  $^{18}\text{F}$ *epi-18*, the labeling conditions could be modified to reduce the basicity and reaction temperature, although such measures would be at the expense of radiochemical yield as vigorous conditions are typically needed for radiofluorination reactions to expedite reaction times and drive the disproportionate stoichiometry. In the literature, epimerization of tadalafil and its derivatives are known to occur with as little as 2–3 equiv of base, such as  $\text{K}_3\text{PO}_4$ , *t*-BuOK, or TBAOH, and at temperatures as low as 28 °C.<sup>32,38,41</sup> We have seen during our initial exploration of radiolabeling conditions that the radiofluorination of precursor **20** requires temperatures over at least 60 °C to proceed (Table 1, entry 5), which suggested that the higher temperatures required for radiofluorination would unavoidably epimerize our radiolabeled product and precursor (Table S1). The tosylate leaving group could be replaced with a more reactive leaving group, such as a 4-nitrobenzenesulfonate (nosylate) or trifluoromethanesulfonate (triflate), to drive the reaction at lower temperatures, but radiofluorination reactions utilizing these leaving groups are still typically performed above 85 °C. Furthermore, the nucleophilic displacement with  $^{18}\text{F}$ fluoride

**Table 1.**  $^{18}\text{F}$ -Radiolabeling Conditions Explored for Labeling **20**

entry	method	solvent	vol ( $\mu\text{L}$ )	% $^{18}\text{F}$ F <sup>-</sup> stock	temp (°C)	time (min)	RCC $^{18}\text{F}$ <i>epi-18</i> (% <sub><i>n</i> = 3</sub> ) <sup>b</sup>
1	A	$\text{CH}_3\text{CN}$	200	20	90	10	7.0 $\pm$ 4.6
2	A	$\text{CH}_3\text{CN}$	200	20	90	20	15.6 $\pm$ 3.1
3	A	DMF	200	20	90	10	0
4	A	DMF	200	20	90	20	0
5	A	$\text{CH}_3\text{CN}$	200	20	60	20	0
6	B	$\text{CH}_3\text{CN}$	200	20	90	20	6.9 $\pm$ 0.6
7	B	$\text{CH}_3\text{CN}$	200	100	90	20	7.2 $\pm$ 2.5
8 <sup>a</sup>	B	$\text{CH}_3\text{CN}$	200	20	90	20	19.8 $\pm$ 3.9
9	C	1,4-dioxane	50	100	120	20	0

<sup>a</sup>Reaction performed in microcentrifuge tube. <sup>b</sup>Radiochemical conversion (RCC) calculated using the amount of n.d.c. radioactivity loaded and collected during HPLC purification.

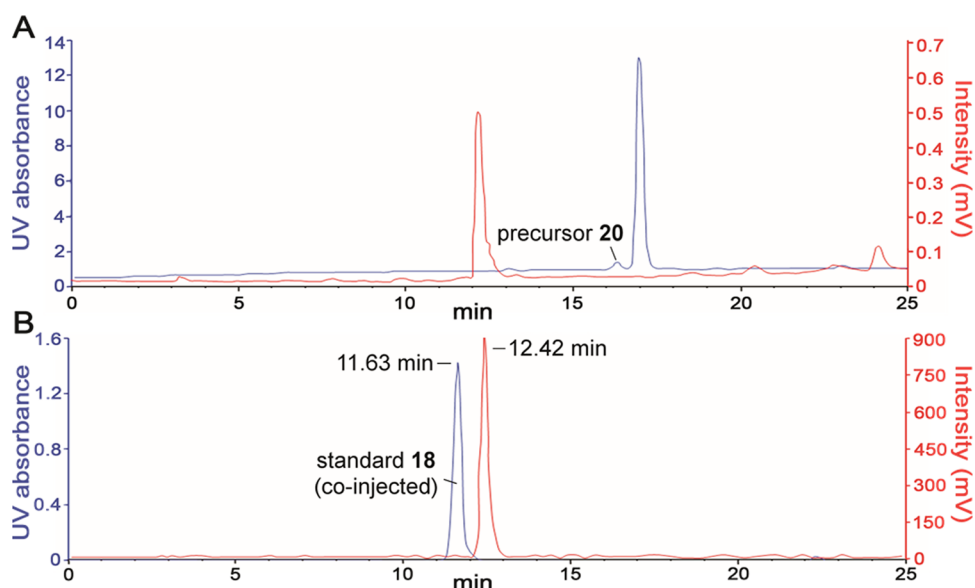
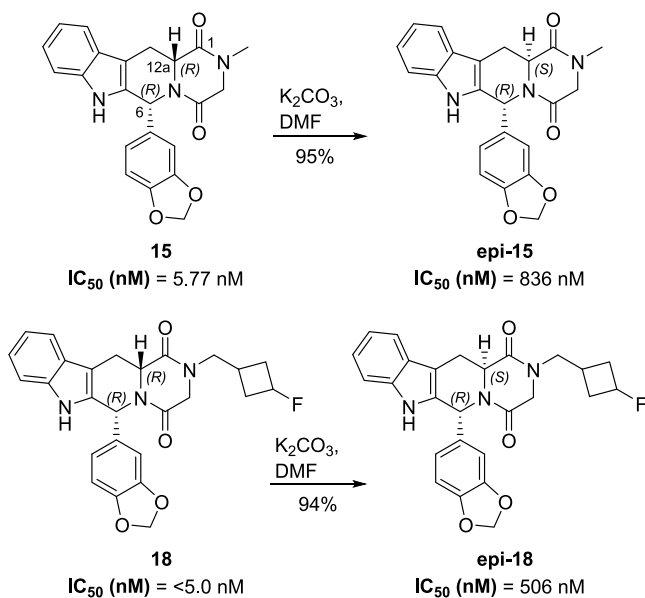


**Figure 4.** HPLC UV and radio-chromatograms from  $^{18}\text{F}$ -labeling of precursor **20**. (A) Purification of reaction mixture (unreacted  $^{18}\text{F}$ fluoride presumably adhered to the column). (B) Quality control (QC) run of collected radio-peak from the purification run, co-injected with standard **18**.

**Scheme 3. Synthesis of (6R,12aS)-Stereoisomers of Compounds 15 and 18 and Their Respective PDE5 Inhibition Values (Transcreeper)**



occurs at a secondary carbon on precursor **20**, which is more challenging to label than a primary carbon, reinforcing the reliance on elevated temperatures to sustain the efficiency of  $^{18}\text{F}$ fluoride substitution.

With reaction temperature ruled out as a variable parameter to manage epimerization, we investigated  $^{18}\text{F}$ TBAF as a less basic substitute for  $^{18}\text{F}$ KF/K<sub>2</sub>CO<sub>3</sub>.  $^{18}\text{F}$ TBAF can be conveniently prepared in situ during the initial processing of  $^{18}\text{F}$ fluoride wherein a solution of tetrabutylammonium bicarbonate (TBA·HCO<sub>3</sub>) is used to elute the trapped  $^{18}\text{F}$ fluoride off the anion exchange cartridge prior to azeotropic drying (Scheme 2, method B). The mildly basic characteristics of the  $^{18}\text{F}$ TBAF/TBA·HCO<sub>3</sub> labeling solution have been recently exploited in the radiosynthesis of  $^{18}\text{F}$ fallypride to reduce side-product formation compared to

the  $^{18}\text{F}$ KF/K<sub>2</sub>CO<sub>3</sub>/K<sub>222</sub> labeling approach.<sup>42</sup> As with our tadalafil radiosynthesis, both  $^{18}\text{F}$ fallypride and its tosylate precursor are base-sensitive, and thus the radiolabeling of precursor **20** may similarly benefit from these mild labeling conditions.

The radiosynthesis with  $^{18}\text{F}$ TBAF/TBA·HCO<sub>3</sub> was performed in a similar manner to that as with the initial  $^{18}\text{F}$ KF/K<sub>2</sub>CO<sub>3</sub>/K<sub>222</sub> labeling complex (Scheme 2, method B). After 20 min reaction time at 90 °C, only the formation of the  $^{18}\text{F}$ epi-**18** product was observed (Figure S1C), with an average radiochemical yield of 6.9% and an  $A_m$  of 52–79 GBq/μmol ( $n = 3$ , EOS), which is comparable to the  $\gamma$   $^{18}\text{F}$ KF/K<sub>2</sub>CO<sub>3</sub>/K<sub>222</sub> system (Table 1, entries 1 and 6). No radiolabeled byproducts were observed (Figure S1A).

The full amount of  $^{18}\text{F}$ TBAF eluted from the anion exchange cartridge was also used to radiolabel precursor **20**, keeping the volumetric ratio the same by resuspending the dried  $^{18}\text{F}$ TBAF in 200 μL of CH<sub>3</sub>CN. The labeling proceeded identically to the aliquot reactions (Table 1, entries 6 and 7), despite a higher concentration of fluoride and increase in the molar ratio of base to precursor (13.5:1, up from 2.76:1 for the aliquot reactions). The labeling reaction was also performed in a microcentrifuge tube to investigate any potential influence of  $^{18}\text{F}$ fluoride adhering to the glass reaction vessel, and interestingly, while the yield of  $^{18}\text{F}$ epi-**18** increased to ~20% (Table 1, entry 8), the reaction mixture contained a plethora of nonradiolabeled byproducts (Figure S1B). The existence of a significant UV absorbance peak associated with an unknown byproduct overlapping with the radio-peak of  $^{18}\text{F}$ epi-**18** precludes this labeling approach from being further utilized.

An acidic method for the radiofluorination of secondary tosylates has been briefly described by Scott and co-workers in the labeling of 3- $^{18}\text{F}$ -cholestene.<sup>43</sup> While the yield was reportedly low, 3.4% n.d.c. HPLC RCY, a nonbasic reaction system, may completely eliminate the epimerization of our radiotracer. In this radiolabeling method (Scheme 2, method C),  $^{18}\text{F}$ HF is first formed by elution of  $^{18}\text{F}$ fluoride from a QMA SepPak with a solution of trifluoroacetic acid (TFA).

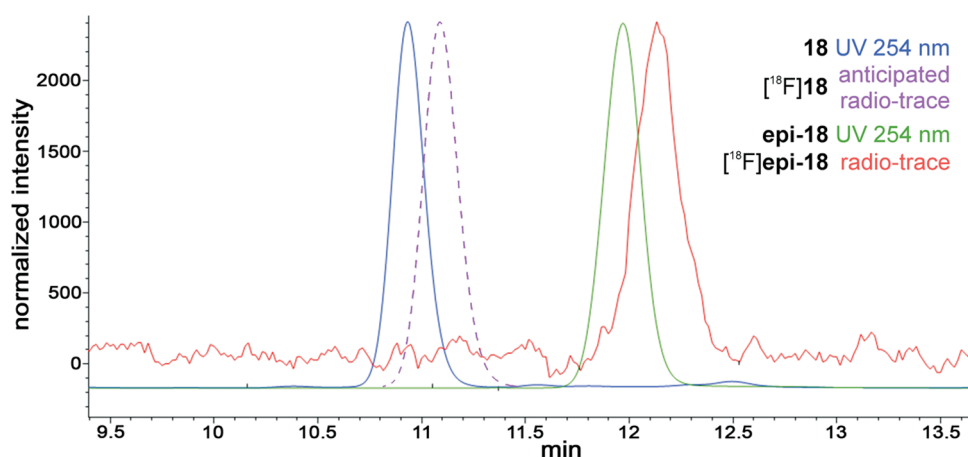


Figure 5. Overlay of HPLC UV and radio-chromatograms of compounds **18**, **epi-18**, and  $[^{18}\text{F}]\text{epi-18}$ .

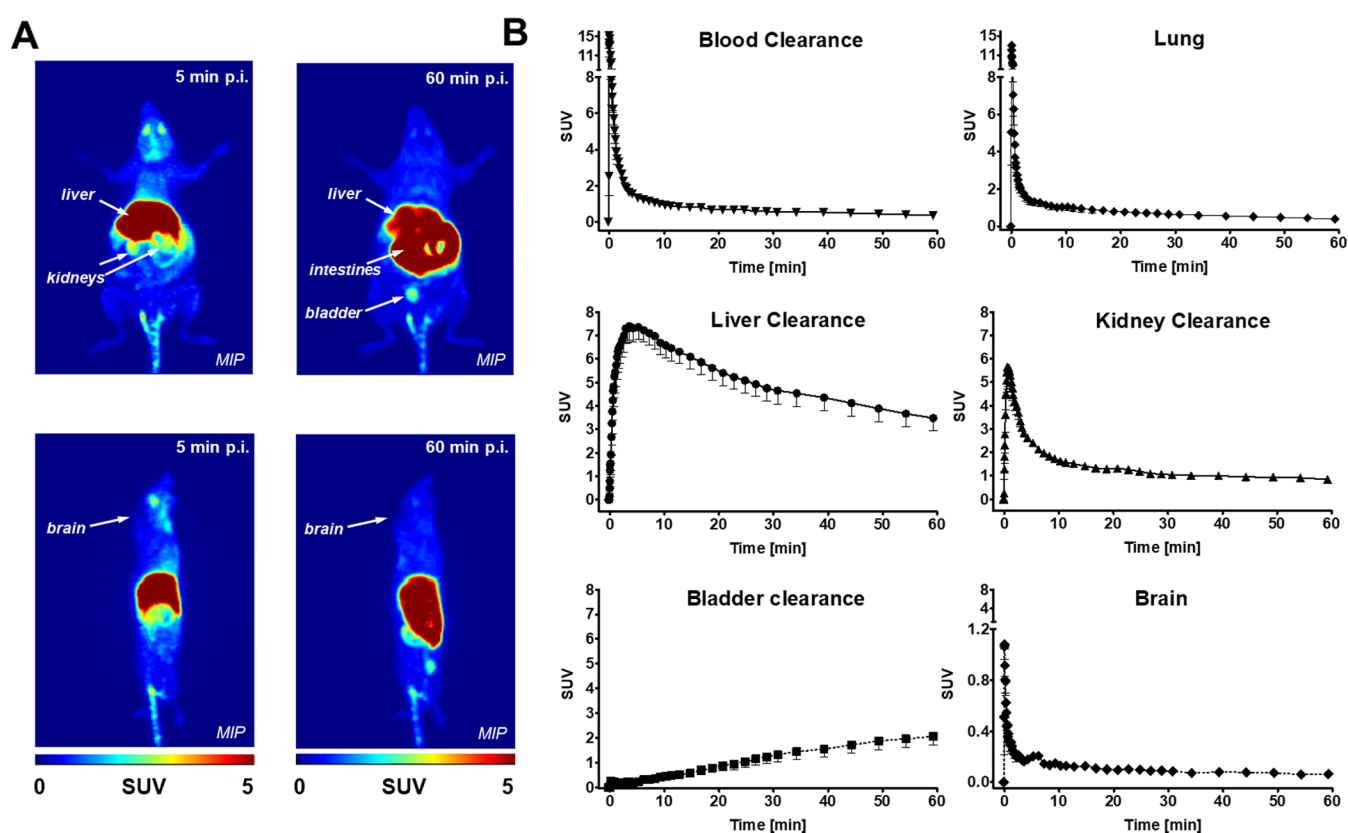


Figure 6. *In vivo* analysis of  $[^{18}\text{F}]\text{epi-18}$  in FVB mice with dynamic PET. (A) Representative PET images from the top and side of a mouse shown as maximum-intensity projections (MIP) at 5 and 60 min p.i. (B) Time–activity curves (TACs) over the entire timeframe of 60 min ( $n = 3$ ) for blood clearance, lung uptake, brain uptake, and clearance through liver, bladder, and kidneys.

This solution is then heated with iron(III) acetylacetonate to trap the  $[^{18}\text{F}]\text{HF}$  and generate an  $[^{18}\text{F}]\text{FeF}$  species, which is then azeotropically dried before resuspension in 1,4-dioxane containing tosylate precursor **20**. In our hands, no radiolabeled products were formed despite multiple attempts at this synthesis.

To further understand how epimerized (6*R*,12*aS*)-stereoisomers of tadalafil and its analogues behave *in vivo*, we evaluated the  $[^{18}\text{F}]\text{epi-18}$  radiotracer in normal FVB mice ( $n = 3$ ) using PET.  $[^{18}\text{F}]\text{epi-18}$  was prepared using the full amount of  $[^{18}\text{F}]\text{TBAF/TBA}\cdot\text{HCO}_3$  (*vide supra*). Immediately following intravenous administration,  $[^{18}\text{F}]\text{epi-18}$  was rapidly cleared

from the systemic blood circulation, as analyzed over the region of the heart (Figure 6A,B). After the first pass,  $[^{18}\text{F}]\text{epi-18}$  showed a low renal but substantial hepatobiliary clearance profile as seen in the time–activity curves (TACs) for the selected organs such as the lung, kidneys, liver, and urinary bladder (Figure 6B). No retention of the radiotracer was observed in the lung, despite the presumably high PEDS target expression.<sup>30</sup> After 60 min p.i., the radiotracer had cleared from most of the peripheral tissues (Figure 6A). There was no skeletal accumulation of  $[^{18}\text{F}]\text{fluoride}$  observed, indicating the pendant  $[^{18}\text{F}]\text{fluorocyclobutyl}$  group of  $[^{18}\text{F}]\text{epi-18}$  was resistant to radiodefluorination *in vivo*.  $[^{18}\text{F}]\text{epi-18}$  may have

passed through the BBB but did not accumulate in the brain over time, resulting in no significant brain uptake.

## CONCLUSIONS

We have attempted to radiolabel an analogue of tadalafil, the first of such efforts since the archetypal PDE5-targeting radiotracer [ $^{11}\text{C}$ ]RAL-01, which remains the only other radiolabeled tadalafil analogue used for PET. However, radiolabeling a precursor molecule containing a 2,5-diketopiperazine ring, such as in the case of tadalafil and its analogues, has proved difficult due to undesired epimerization about the C12a stereocenter. As 2,5-diketopiperazines readily epimerize under basic, acidic, and thermal conditions,<sup>44</sup> the very conditions which are routinely found necessary to drive radiolabeling reactions, tadalafil is not a suitable candidate scaffold to base the design of a radiotracer from. Given our findings, the poor imaging results of [ $^{11}\text{C}$ ]RAL-01 may be the result of epimerization occurring during the basic [ $^{11}\text{C}$ ]-methylation radiolabeling, though it should be noted that while [ $^{11}\text{C}$ ]RAL-01 is a derivative of tadalafil, it bears a hydantoin heterocycle in place of the diketopiperazine and may be of increased stability. Use of  $^{18}\text{F}$ -prosthetic group chemistry may be an alternative strategy to avoid subjecting a tadalafil-based precursor to harsh  $^{18}\text{F}$ -radiofluorination conditions and avoid epimerization.

## EXPERIMENTAL SECTION

**General Chemistry Procedures.** All chemicals and reagents were purchased from commercial suppliers, including Sigma-Aldrich, Fisher Scientific, Oakwood Chemical, and Synthonyx, and used without further purification. Room temperature (rt) refers to 20–25 °C. Reaction monitoring was performed using thin-layer chromatography (TLC) on silica 60 F254 plates and visualized with UV light or ethanolic anisaldehyde stain. Flash chromatography was performed using SilicaFlash F60, 40–63  $\mu\text{m}$  silica gel. NMR spectra were recorded on an Agilent/Varian Inova four-channel 500 MHz spectrometer at room temperature. All chemical shifts are reported in parts per million (ppm). High-resolution mass spectrometry (HRMS) was performed on an Agilent Technologies 6220 orthogonal acceleration TOF instrument. Final compounds tested for biological assays or imaging studies were >95% pure (HPLC).

**In Vitro Inhibition Assays.** Inhibition assays were performed by Reaction Biology Corp. (Malvern) using the Transcreeper AMP<sup>2</sup>/GMP<sup>2</sup> fluorescence polarization assay. Transcreeper quantitatively measures the ability of a compound to inhibit cGMP hydrolysis by detecting the GMP produced by PDE5. Free GMP displaces a fluorescent tracer from GMP-specific antibody resulting in a quantitative change in fluorescent properties. In brief, compounds **15–18** and **epi-18** were dissolved in dimethyl sulfoxide (DMSO) to a concentration of 20 mM and were tested in a 10-dose IC<sub>50</sub> assay with threefold serial dilution, starting at 100  $\mu\text{M}$ . Human recombinant PDE5A enzyme solution was dissolved in assay buffer containing 10 mM Tris (pH 7.5), 5 mM MgCl<sub>2</sub>, 0.01% Brij-35, 1 mM dithiothreitol (DTT), and 1% DMSO. Test compounds in DMSO were added to the enzyme mixture and the assay started upon addition of 1  $\mu\text{M}$  cGMP substrate solution. After incubation for 1 h stop buffer, consisting of 100 nM *N*-(2-hydroxyethyl)piperazine-*N'*-ethanesulfonic acid (HEPES), 0.2% Brij-35, and 500 nM ethylenediaminetetra-

acetic acid (EDTA) (pH 7.5), and the GMP detection mixture, consisting of 50 mM Tris (pH 7.5), 16 nM AMP/GMP AlexaFluor 633 tracer, and variable AMP<sup>2</sup>/GMP<sup>2</sup> antibody, were added. After 90 min incubation, the fluorescence polarization was measured (excitation: 620 nm, emission: 688 nm). A control compound, methoxyquinazoline, was tested in a 10-dose IC<sub>50</sub> assay with threefold serial dilution starting at 50 nM. Data was analyzed based on a GMP standard curve to obtain the amount of GMP produced. Curve fits for % enzyme activity (relative to DMSO controls) for each compound were performed with GraphPad Prism software to determine IC<sub>50</sub>.

**General Radiochemistry Procedures.** No-carrier-added [ $^{18}\text{F}$ ]fluoride was produced using either a TR19/9 or TR24 cyclotron (Advanced Cyclotron Systems, Inc., Canada) through the  $^{18}\text{O}(\text{p},\text{n})^{18}\text{F}$  nuclear reaction by irradiation of [ $^{18}\text{O}$ ]H<sub>2</sub>O (98%, 3.0 mL; Rotem Industries, Germany). Radio-TLC was performed on silica 60 F254 plates and visualized using a Bioscan AR-2000 radio-TLC scanner. Activity was measured using a Biodex Atomlab 400 or 500 dose calibrator. Semipreparative HPLC of radiolabeled compounds was performed on either a Gilson HPLC system (Mandel Scientific, Canada) equipped with a 321 pump, a 155 UV/vis dual-wavelength detector, and a Berthold (Germany) HERM radiometric detector, or an Agilent 1260 series HPLC system equipped with a quaternary pump, a VWD detector, and a Raytest (Germany) Gabi radioactivity flow monitor. Both HPLC systems were equipped with a Rheodyne 7725 injection valve with a 2 mL injection loop. UV absorbance was monitored at 210 and 254 nm wavelength. Semipreparative HPLC was performed using a Phenomenex C18 column (Luna 5  $\mu\text{m}$ , 100 Å, 250  $\times$  10 mm<sup>2</sup>) using a gradient of solvent A: H<sub>2</sub>O and solvent B: CH<sub>3</sub>CN (0–4.5 min: isocratic 60% B, 4.5–18 min: linear gradient to 80% B, 18–21 min: linear gradient to 95% B, 21–25 min: isocratic 95% B) at a flow rate of 3.0 mL/min. Molar activities were determined by dividing the amount of radioactivity collected in the radiotracer peak from HPLC, divided by the molar amount obtained by referencing the UV absorbance of the collected fraction by use of a calibration curve for **epi-6**. Non-decay-corrected radiochemical yield was calculated as the fraction of radioactivity isolated after HPLC purification divided by the amount of radioactivity injected for HPLC purification.

**PET Imaging Experiments.** All animal experiments were carried out in accordance with guidelines of the Canadian Council on Animal Care (CCAC) and approved by the local animal care committee of the Cross Cancer Institute. Normal FVB mice (Charles-River, QC, Canada) were anesthetized with isoflurane (40% O<sub>2</sub>, 60% N<sub>2</sub>) and their body temperature was kept constant at 37 °C. Mice were positioned and immobilized in prone position into the center of the field of view of an INVEON PET scanner (Siemens Preclinical Solutions, Knoxville, TN). Radioactivity amount (4–8 MBq in 100–150  $\mu\text{L}$  of saline) was determined using a dose calibrator (Atomlab 300, Biodex Medical Systems, New York, NY) and injected through a tail vein catheter. Dynamic PET data acquisition was performed in the 3D list mode for 60 min. Dynamic list mode data were sorted into sinograms with 54-time frames (10  $\times$  2, 8  $\times$  5, 6  $\times$  10, 6  $\times$  20, 8  $\times$  60, 10  $\times$  120, 5  $\times$  300 s). Image frames were reconstructed using ordered subset expectation maximization (OSEM) or maximum a posteriori (MAP) reconstruction modes. Image files were further processed using the ROVER v2.0.51 software (ABX

GmbH, Radeberg, Germany). Masks defining 3D regions of interest (ROI) were set and defined by 50% thresholding. Mean standardized uptake values [ $SUV_{\text{mean}} = (\text{activity/mL tissue})/(\text{injected activity/body weight})$ ] were generated for each ROI, and time–activity curves (TAC) were constructed using GraphPad Prism 4.0 (GraphPad Software, La Jolla, CA).

**Statistical Analysis.** All semiquantified PET data are expressed as mean  $\pm$  standard error of the mean (SEM) from  $n$  experiments. Where applicable, statistical differences were tested by Student's  $t$ -test and were considered significant for  $p < 0.05$  (\*),  $p < 0.01$  (\*\*), and  $p < 0.001$  (\*\*\*)

**Docking Study.** Molecular docking simulations of compounds **16–18** were performed using the FITTED 1.5 program (FORECASTER platform) with the X-ray cocrystal structure of the catalytic domain of PDE5 in complex with tadalafil (PDB: 1XOZ).<sup>45</sup> The resulting docked structures and figures were prepared using PyMOL.

**Preparation of Compounds.** **Compound 13.** To a solution of *d*-tryptophan methyl ester hydrochloride (3.27 g, 12.94 mmol) and piperonal (2.12 g, 14.12 mmol, 1.09 equiv) in  $\text{CH}_3\text{CN}$  (40 mL) was added HCl (37%, five drops). The reaction was heated to 80 °C and monitored *via* TLC. The stereochemical outcome is controlled by the CIAT process, taking advantage of the low solubility of the desired (1*R*,3*R*)-isomer when acetonitrile ( $\text{CH}_3\text{CN}$ ) is used as the reaction solvent.<sup>38</sup> During the reaction, the (1*S*,3*R*)- and (1*R*,3*R*)-isomers are initially formed in almost equal amounts and are in a state of acid-catalyzed epimerization equilibrium. As the desired (1*R*,3*R*)-isomer precipitates out of solution due to its low solubility in  $\text{CH}_3\text{CN}$ , the epimerization equilibrium is continuously driven toward the desired (1*R*,3*R*)-isomer until all of the (1*S*,3*R*)-isomer has epimerized. After 64 h, the reaction mixture was cooled to room temp and then to 0 °C. The slightly tan precipitate was collected using vacuum filtration with a Büchner funnel and washed with cold  $\text{CH}_3\text{CN}$ . The product was dried to obtain **13** as a lightly tan powder (4.66 g, 12.06 mmol, 93%).  $R_f$  (1:1 hexanes/EtOAc) = 0.39;  $^1\text{H}$  NMR (498 MHz,  $\text{CDCl}_3$ ):  $\delta$  = 7.56 (d, 1H,  $J$  = 7.29 Hz, H-5), 7.48 (br. s., 1H, NH), 7.25 (d, 1H,  $J$  = 7.47 Hz, H-8), 7.18 (dt, 1H,  $J$  = 1.09, 7.10 Hz, H-6), 7.14 (dt, 1H,  $J$  = 0.90, 7.10 Hz, H-7), 6.91 (dd, 1H,  $J$  = 1.46, 7.84 Hz, H-10), 6.86 (d, 1H,  $J$  = 1.28 Hz, H-12), 6.83 (d, 1H,  $J$  = 7.84 Hz, H-11), 5.98 (s, 2H,  $\text{O}_2\text{CH}_2$ ), 5.20 (s, 1H, H-1), 3.98 (dd, 1H,  $J$  = 4.19, 11.12 Hz, H-3), 3.84 (s, 3H,  $\text{OCH}_3$ ), 3.24 (ddd, 1H,  $J$  = 1.64, 4.01, 14.94 Hz, H-4a), 3.02 (ddd, 1H,  $J$  = 2.50, 11.20, 15.00 Hz, H-4b) ppm;  $^{13}\text{C}$  NMR (125 MHz,  $\text{CDCl}_3$ ):  $\delta$  = 173.11 (C=O), 148.23 ( $\text{C}_{\text{Ar}}$ ), 147.87 ( $\text{C}_{\text{Ar}}$ ), 136.15 ( $\text{C}_{\text{Ar}}$ ), 134.67 ( $\text{C}_{\text{Ar}}$ ), 134.61 ( $\text{C}_{\text{Ar}}$ ), 127.14 ( $\text{C}_{\text{Ar}}$ ), 122.01 ( $\text{CH}_{\text{Ar}}$ ), 121.97 ( $\text{CH}_{\text{Ar}}$ ), 119.67 ( $\text{CH}_{\text{Ar}}$ ), 118.24 ( $\text{CH}_{\text{Ar}}$ ), 110.92 ( $\text{CH}_{\text{Ar}}$ ), 108.90 ( $\text{C}_{\text{Ar}}$ ), 108.78 ( $\text{CH}_{\text{Ar}}$ ), 108.32 ( $\text{CH}_{\text{Ar}}$ ), 101.22 ( $\text{OCH}_2\text{O}$ ), 58.43 (CH), 56.87 (CH), 52.26 ( $\text{OCH}_3$ ), 25.63 (C-4); HRMS (EI)  $m/z$ :  $[M + H]^+$  calcd for  $\text{C}_{20}\text{H}_{19}\text{N}_2\text{O}_4$  351.1339, found 351.1338.

**Compound 14.** To a vigorously stirred 0 °C solution of the *cis*-tetrahydro- $\beta$ -carboline **13** (1.77 g, 4.58 mmol) and chloroacetyl chloride (0.81 mL, 10.18 mmol, 2.2 equiv) in dichloromethane (DCM) (20 mL) and water (10 mL) was added  $\text{NaHCO}_3$  (0.95 g, 11.31 mmol, 2.5 equiv). After 1 h the reaction mixture was diluted with DCM (20 mL) and the aqueous layer removed. The organic was washed with water and brine, then dried over  $\text{Na}_2\text{SO}_4$  and concentrated *in vacuo*. The crude yellow solid was purified *via* recrystallization in MeOH to yield **14** as a light yellow crystals (1.70 g, 3.98 mmol,

87% yield), comparable to the literature reference.<sup>46</sup>  $R_f$  (6:4 hexanes/EtOAc) = 0.55;  $^1\text{H}$  NMR (400 MHz,  $\text{CDCl}_3$ ):  $\delta$  = 7.75 (br. s., 1H, NH), 7.60 (d, 1H,  $J$  = 7.63 Hz, H-5), 7.29 (d, 1H,  $J$  = 7.63 Hz, H-8), 7.21 (t, 1H,  $J$  = 7.41 Hz, H-6), 7.17 (t, 1H,  $J$  = 7.30 Hz, H-7), 6.79–6.95 (m, 1.5H,  $\text{H}_{\text{Ar}}$ ), 6.66 (br. s., 1.5H,  $\text{H}_{\text{Ar}}$ ), 5.91 (s, 2H,  $\text{O}_2\text{CH}_2$ ), 4.95 (br. s., 1H, H-1), 4.35 (d, 1H,  $J$  = 12.30 Hz,  $\text{CH}_2\text{Cl}$ ), 4.21 (d, 1H,  $J$  = 12.32 Hz,  $\text{CH}_2\text{Cl}$ ), 3.69 (d, 1H,  $J$  = 15.85 Hz, H-3), 3.22 (br. s., 3H,  $\text{CH}_3$ ), 3.15–3.22 (m, 2H, H-4); HRMS (EI)  $m/z$ :  $[M + H]^+$  calcd for  $\text{C}_{22}\text{H}_{20}\text{ClN}_2\text{O}_5$  426.0982, found 427.1057.

**Compound 15.** To a solution of chloroacetyl *cis*-tetrahydro- $\beta$ -carboline **14** (0.180 g, 0.422 mmol) in DMF (6 mL) was added an ethanolic solution of methylamine (33 wt %, 65 mg, 0.69 mmol, 1.6 equiv). The reaction was monitored by TLC and continued overnight at rt. Upon completion, the reaction was diluted with  $\text{H}_2\text{O}$  (40 mL), and a white ppt formed. The reaction mixture was chilled overnight in the fridge and then the solid ppt was filtered off and dried with a stream of air. The product was recrystallized with glacial acetic acid to yield tadalafil **15** as a white crystalline solid (0.150 g, 0.385 mmol, 91% yield).  $R_f$  (1:9 hexanes/EtOAc) = 0.19;  $^1\text{H}$  NMR (498 MHz,  $\text{DMSO}-d_6$ ):  $\delta$  = 11.00 (s, 1H, NH), 7.53 (d, 1H,  $J$  = 7.75 Hz, H-11), 7.28 (d, 1H,  $J$  = 8.01 Hz, H-8), 7.04 (t, 1H,  $J$  = 8.01 Hz, H-9), 6.98 (t, 1H,  $J$  = 7.24 Hz, H-10), 6.85 (s, 1H, H-2'), 6.73–6.79 (m, 2H, H-5'/6'), 6.12 (s, 1H, H-6), 5.90 (s, 2H, H-7'), 4.38 (dd, 1H,  $J$  = 4.26, 11.63 Hz, H-12a), 4.16 (d, 1H,  $J$  = 17.06 Hz, H-3), 3.93 (d, 1H,  $J$  = 17.06 Hz, H-3), 3.50 (dd, 1H,  $J$  = 4.52, 15.76 Hz, H-12), 2.95 (dd, 1H,  $J$  = 12.15, 15.76 Hz, H-12), 2.91 (s, 3H, H-13), 1.89 (s, 0.23H, AcOH) ppm;  $^{13}\text{C}$  NMR (125 MHz,  $\text{DMSO}-d_6$ ):  $\delta$  = 167.32 (C=O), 167.00 (C=O), 147.47 ( $\text{C}_{\text{Ar}}$ ), 146.50 ( $\text{C}_{\text{Ar}}$ ), 137.41 ( $\text{C}_{\text{Ar}}$ ), 136.64 ( $\text{C}_{\text{Ar}}$ ), 134.38 ( $\text{C}_{\text{Ar}}$ ), 126.21 ( $\text{C}_{\text{Ar}}$ ), 121.67 (C-9), 119.75 (C-10), 119.30 (C-6'), 118.54 (C-11), 111.75 (C-8), 108.42 (C-5'), 107.41 (C-2'), 105.20 ( $\text{C}_{\text{Ar}}$ ), 101.34 (C-7'), 55.96 (C-12a), 55.72 (C-6), 51.92 (C-3), 33.33 (C-13), 23.57 (C-12) ppm; HRMS (EI)  $m/z$ :  $[M + \text{Na}]^+$  calcd for  $\text{C}_{22}\text{H}_{19}\text{N}_3\text{NaO}_4$  412.1268, found 412.1265.

**Compound epi-15.** To a solution of tadalafil **15** (11.5 mg, 29.5  $\mu\text{mol}$ ) in DMF (100  $\mu\text{L}$ ) was added an aqueous solution of saturated  $\text{K}_2\text{CO}_3$  (20  $\mu\text{L}$ ). The reaction mixture was heated to 130 °C for 10 min, then cooled to rt, diluted with  $\text{CH}_3\text{CN}$  and  $\text{H}_2\text{O}$  (3:2, 0.5 mL), and purified *via* semipreparative HPLC using conditions described in the [General Radiochemistry Procedures](#) section. The product eluting at 7.5 min was collected and lyophilized to yield **epi-15** as a white powder (10.9 mg, 28.0  $\mu\text{mol}$ , 95% yield).  $R_f$  (1:9 hexanes/EtOAc) = 0.29;  $^1\text{H}$  NMR (498 MHz,  $\text{DMSO}-d_6$ ):  $\delta$  = 7.49 (d, 1H,  $J$  = 7.87 Hz, H-11), 7.31 (d, 1H,  $J$  = 8.06 Hz, H-8), 7.10 (t, 1H,  $J$  = 7.51 Hz, H-9), 7.01 (t, 1H,  $J$  = 7.51 Hz, H-10), 6.86 (d, 1H,  $J$  = 8.06 Hz, H-6'), 6.82 (s, 1H, H-6), 6.76 (m, 1H, H-2'), 6.60 (d, 1H,  $J$  = 8.06 Hz, H-5'), 5.99 (d, 2H,  $J$  = 6.23 Hz, H-7'), 4.24 (d, 1H,  $J$  = 17.58 Hz, H-3), 4.07 (dd, 1H,  $J$  = 4.03, 11.90 Hz, H-12a), 4.03 (d, 1H,  $J$  = 17.95 Hz, H-3), 3.25 (dd, 1H,  $J$  = 4.21, 15.38 Hz, H-12), 2.95 (dd, 1H,  $J$  = 12.27, 14.83 Hz, H-12), 2.84 (s, 3H, H-13) ppm;  $^{13}\text{C}$  NMR (126 MHz,  $\text{DMSO}-d_6$ ):  $\delta$  = 164.60 (C=O), 162.22 (C=O), 147.58 ( $\text{C}_{\text{Ar}}$ ), 147.20 ( $\text{C}_{\text{Ar}}$ ), 136.21 ( $\text{C}_{\text{Ar}}$ ), 132.85 ( $\text{C}_{\text{Ar}}$ ), 130.30 ( $\text{C}_{\text{Ar}}$ ), 125.86 ( $\text{C}_{\text{Ar}}$ ), 121.66 (C-9/11), 121.62 (C-9/11), 118.83 (C-10), 118.07 (C-6'), 111.28 (C-8), 108.29 (C-5'), 108.11 (C-2'), 107.46 ( $\text{C}_{\text{Ar}}$ ), 101.21 (C-7'), 51.96 (C-12a), 50.79 (C-6), 50.63 (C-3), 32.57 (C-13), 26.65 (C-12) ppm; HRMS (EI)  $m/z$ :  $[M + \text{Na}]^+$  calcd for  $\text{C}_{22}\text{H}_{19}\text{N}_3\text{NaO}_4$  412.1268, found 412.1263.

**Compound 16.** To a solution of chloroacetyl *cis*-tetrahydro- $\beta$ -carboline **14** (51 mg, 0.12 mmol) in DMF (5 mL) were added 2-fluoroethylamine hydrochloride (59 mg, 0.59 mmol, 4.9 equiv) and  $\text{Cs}_2\text{CO}_3$  (90 mg, 0.28 mmol, 2.3 equiv). The reaction mixture was stirred at rt over the weekend, and the solvent was then removed at 60 °C on a rotovap. The crude mixture was resuspended in DCM, and a white powder (fluoroethylamine) precipitated out that was removed by filtration. The yellow DCM solution was purified *via* flash chromatography (1:1 hexanes/EtOAc) to yield a light yellow powder, which was further purified *via* recrystallization in acetic acid and  $\text{H}_2\text{O}$ , and washed with cold EtOH/ $\text{H}_2\text{O}$  to yield **16** as a white powder (28.8 mg, 68.3  $\mu\text{mol}$ , 57% yield).  $R_f$  (1:1 hexanes/EtOAc) = 0.20;  $^1\text{H}$  NMR (500 MHz,  $\text{DMSO}-d_6$ ):  $\delta$  = 7.54 (d, 1H,  $J$  = 7.89 Hz, H-11), 7.30 (d, 1H,  $J$  = 8.07 Hz, H-8), 7.05 (t, 1H,  $J$  = 7.60 Hz, H-9), 6.99 (t, 1H,  $J$  = 7.20 Hz, H-10), 6.84 (s, 1H, H-2'), 6.76 (m, 2H, H-5'/6'), 6.17 (s, 1H, H-6), 5.92 (s, 2H, H-7'), 4.60 (td, 2H,  $J$  = 5.10 Hz,  $^2J_{\text{H-F}}$  = 47.50 Hz,  $\text{CH}_2\text{F}$ ), 4.47 (dd, 1H,  $J$  = 4.59, 11.55 Hz, H-12a), 4.27 (d, 1H,  $J$  = 16.87 Hz, H-3), 4.01 (d, 1H,  $J$  = 17.06 Hz, H-3), 3.85 (tdd, 1H,  $J$  = 4.60, 14.86 Hz,  $^3J_{\text{H-F}}$  = 28.60 Hz,  $\text{CH}_2\text{CH}_2\text{F}$ ), 3.64 (tdd, 1H,  $J$  = 5.00, 15.20 Hz,  $^3J_{\text{H-F}}$  = 25.50 Hz,  $\text{CH}_2\text{CH}_2\text{F}$ ), 3.49 (dd, 1H,  $J$  = 4.77, 15.77 Hz, H-12), 2.97 (dd, 1H,  $J$  = 11.83, 15.50 Hz, H-12) ppm;  $^{13}\text{C}$  NMR (126 MHz,  $\text{DMSO}-d_6$ ):  $\delta$  = 167.13 (C=O), 167.10 (C=O), 147.06 ( $\text{C}_{\text{Ar}}$ ), 146.09 ( $\text{C}_{\text{Ar}}$ ), 136.70 ( $\text{C}_{\text{Ar}}$ ), 136.11 ( $\text{C}_{\text{Ar}}$ ), 133.84 ( $\text{C}_{\text{Ar}}$ ), 125.70 ( $\text{C}_{\text{Ar}}$ ), 121.23 ( $\text{CH}_{\text{Ar}}$ ), 119.19 ( $\text{CH}_{\text{Ar}}$ ), 118.85 ( $\text{CH}_{\text{Ar}}$ ), 118.08 ( $\text{CH}_{\text{Ar}}$ ), 111.30 ( $\text{CH}_{\text{Ar}}$ ), 107.98 ( $\text{CH}_{\text{Ar}}$ ), 106.83 ( $\text{CH}_{\text{Ar}}$ ), 104.54 ( $\text{C}_{\text{Ar}}$ ), 100.89 (C-7'), 81.56 (d,  $^1J_{\text{C-F}}$  = 166.2 Hz,  $\text{CH}_2\text{F}$ ), 55.33 and 54.91 (C-6/12a), 50.69 (C-3), 45.77 (d,  $^2J_{\text{C-F}}$  = 19.6 Hz,  $\text{CH}_2\text{CH}_2\text{F}$ ), 22.57 (C-12) ppm; HRMS (EI)  $m/z$ :  $[\text{M} + \text{Na}]^+$  calcd for  $\text{C}_{23}\text{H}_{20}\text{FN}_3\text{NaO}_4$  444.1330, found 444.1326.

**Compound 17.** To a solution of chloroacetyl *cis*-tetrahydro- $\beta$ -carboline **14** (101 mg, 0.237 mmol) in DMF (6 mL) were added 3-fluorocyclobutylamine hydrochloride (40 mg, 0.45 mmol, 1.9 equiv) and  $\text{Cs}_2\text{CO}_3$  (77 mg, 0.24 mmol, 1 equiv). After 24 h stirring at rt,  $\text{H}_2\text{O}$  (30 mL) was added to the reaction mixture and a white ppt crashed out of solution that was collected *via* vacuum filtration. The crude powder was purified *via* flash chromatography (6:4  $\rightarrow$  1:1 hexanes/EtOAc) to yield **17** as a white solid (73 mg, 0.16 mmol, 68% yield) with an approximate 7:3 ratio of *cis/trans*-fluorocyclobutylamine product.  $R_f$  (1:9 hexanes/EtOAc) = 0.40;  $^1\text{H}$  NMR (498 MHz,  $\text{CDCl}_3$ ):  $\delta$  = 7.85 (br. s., 1H, NH), 7.62 (d, 1H,  $J$  = 7.51 Hz, H-11), 7.29 (m, 1H, H-8), 7.12–7.25 (m, 2H, H-9/10), 6.88 (m, 1H, H-2'), 6.69–6.78 (m, 2H, H-5'/6'), 6.20 (m, 1H, H-6), 5.89 (m, 1H, H-7'), 5.13–5.31 (m, 0.27H,  $\text{CHF}_{\text{trans}}$ ), 5.18 (quin, 0.27H,  $J$  = 8.50 Hz,  $\text{NCH}_{\text{trans}}$ ), 4.86 (quin, 0.71H,  $J$  = 6.60 Hz,  $^2J_{\text{H-F}}$  = 55.67 Hz,  $\text{CHF}_{\text{cis}}$ ), 4.54 (tt, 0.71H,  $J$  = 7.8, 9.5 Hz,  $\text{NCH}_{\text{cis}}$ ), 4.31 (m, 1H, H-12a), 4.14 (d, 0.71H,  $J$  = 17.21 Hz, H-3), 3.99 (m, 1.27H, H-3), 3.75 (dd, 1H,  $J$  = 4.58, 15.93 Hz, H-12), 3.24 (dd, 1H,  $J$  = 11.63, 15.29 Hz, H-12), 2.70–2.84 (m, 1.45H,  $(\text{CH}_2)_2\text{CHF}_{\text{cis}}$ ), 2.50–2.68 (m, 1.11H,  $(\text{CH}_2)_2\text{CHF}_{\text{trans}}$ ), 2.24–2.50 (m, 1.45H,  $(\text{CH}_2)_2\text{CHF}_{\text{cis}}$ ) ppm;  $^{13}\text{C}$  NMR (125 MHz,  $\text{CDCl}_3$ ):  $\delta$  = 167.02 (C=O), 166.82 (C=O), 147.91 ( $\text{C}_{\text{Ar}}$ ), 147.25 ( $\text{C}_{\text{Ar}}$ ), 136.53 ( $\text{C}_{\text{Ar}}$ ), 135.02 ( $\text{C}_{\text{Ar}}$ ), 132.73 ( $\text{C}_{\text{Ar}}$ ), 126.15 ( $\text{C}_{\text{Ar}}$ ), 122.64 ( $\text{CH}_{\text{Ar}}$ ), 120.94 ( $\text{CH}_{\text{Ar}}$ ), 120.21 ( $\text{CH}_{\text{Ar}}$ ), 118.60 ( $\text{CH}_{\text{Ar}}$ ), 111.22 ( $\text{CH}_{\text{Ar}}$ ), 108.26 ( $\text{CH}_{\text{Ar}}$ ), 107.55 ( $\text{CH}_{\text{Ar}}$ ), 106.47 ( $\text{C}_{\text{Ar}}$ ), 101.20 (C-7'), 81.05 (d,  $^1J_{\text{C-F}}$  = 212.7 Hz,  $\text{CHF}$ ), 56.58, 56.46, and 56.42 (C-6, C-12a,  $\text{NCH}(\text{CH}_2)_2$ ), 45.86 (C-3), 35.90 (d,  $^2J_{\text{C-F}}$  = 20.1 Hz,  $(\text{CH}_2)_2\text{CHF}$ ), 35.86

(d,  $^2J_{\text{C-F}}$  = 20.6 Hz,  $(\text{CH}_2)_2\text{CHF}$ ), 23.54 (C-12) ppm; HRMS (EI)  $m/z$ :  $[\text{M} + \text{Na}]^+$  calcd for  $\text{C}_{25}\text{H}_{22}\text{FN}_3\text{NaO}_4$  470.1487, found 470.1484.

**Compound 18.** To a solution of chloroacetyl *cis*-tetrahydro- $\beta$ -carboline **14** (103 mg, 0.241 mmol) in DMF (6 mL) were added (3-fluorocyclobutyl)methylamine hydrochloride (36 mg, 0.26 mmol, 1.1 equiv) and  $\text{Cs}_2\text{CO}_3$  (79 mg, 0.24 mmol, 1 equiv). After 24 h stirring at rt,  $\text{H}_2\text{O}$  (30 mL) was added to the reaction mixture and a white ppt crashed out of solution that was collected *via* vacuum filtration. The crude powder was purified *via* flash chromatography (1:1  $\rightarrow$  4:6 hexanes/EtOAc) to yield **18** as a white solid (68 mg, 0.15 mmol, 61% yield).  $R_f$  (1:9 hexanes/EtOAc) = 0.44;  $^1\text{H}$  NMR (498 MHz,  $\text{CDCl}_3$ ):  $\delta$  = 7.81 (s, 1H, NH), 7.63 (d, 1H,  $J$  = 7.51 Hz, H-11), 7.30 (d, 1H,  $J$  = 7.51 Hz, H-8), 7.15–7.25 (m, 2H, H-9/10), 6.86 (dd, 1H,  $J$  = 1.56, 7.97 Hz, H-2'), 6.73 (m, 2H, H-5'/6'), 6.20 (s, 1H, H-6), 5.90 (m, 2H, H-7'), 5.21 (quin, 1H,  $J$  = 5.90,  $^2J_{\text{H-F}}$  = 55.67 Hz,  $\text{CHF}$ ), 4.34 (dd, 1H,  $J$  = 4.49, 11.45 Hz, H-12a), 4.09 (d, 1H,  $J$  = 17.20 Hz, H-3), 3.93 (d, 1H,  $J$  = 17.40 Hz, H-3), 3.77 (dd, 1H,  $J$  = 4.49, 16.02 Hz, H-12), 3.73 (dd, 1H,  $J$  = 8.33, 13.83 Hz,  $\text{NCH}_2\text{CH}$ ), 3.43 (dd, 1H,  $J$  = 7.97, 13.83 Hz,  $\text{NCH}_2\text{CH}$ ), 3.24 (dd, 1H,  $J$  = 11.81, 15.66 Hz, H-12), 2.64–2.75 (m, 1H,  $\text{NCH}_2\text{CH}$ ), 2.31–2.46 (m, 2H,  $(\text{CH}_2)_2\text{CHF}$ ), 2.15–2.28 (m, 2H,  $(\text{CH}_2)_2\text{CHF}$ ) ppm;  $^{13}\text{C}$  NMR (125 MHz,  $\text{CDCl}_3$ ):  $\delta$  = 166.99 (C=O), 166.84 (C=O), 147.88 ( $\text{C}_{\text{Ar}}$ ), 147.16 ( $\text{C}_{\text{Ar}}$ ), 136.52 ( $\text{C}_{\text{Ar}}$ ), 135.18 ( $\text{C}_{\text{Ar}}$ ), 132.80 ( $\text{C}_{\text{Ar}}$ ), 126.15 ( $\text{C}_{\text{Ar}}$ ), 122.50 ( $\text{CH}_{\text{Ar}}$ ), 120.54 ( $\text{CH}_{\text{Ar}}$ ), 120.11 ( $\text{CH}_{\text{Ar}}$ ), 118.58 ( $\text{CH}_{\text{Ar}}$ ), 111.25 ( $\text{CH}_{\text{Ar}}$ ), 108.24 ( $\text{CH}_{\text{Ar}}$ ), 107.39 ( $\text{CH}_{\text{Ar}}$ ), 106.36 ( $\text{C}_{\text{Ar}}$ ), 101.19 (C-7'), 87.19 (d,  $^1J_{\text{C-F}}$  = 205.7 Hz,  $\text{CHF}$ ), 56.38 and 56.16 (C-6/12a), 50.45, 50.43, and 50.37 (2  $\times$   $\text{NCH}_2\text{CH}$ , C-3), 33.86 (d,  $^2J_{\text{C-F}}$  = 21.7 Hz,  $(\text{CH}_2)_2\text{CHF}$ ), 33.71 (d,  $^2J_{\text{C-F}}$  = 21.9 Hz,  $(\text{CH}_2)_2\text{CHF}$ ), 25.75 (d,  $^3J_{\text{C-F}}$  = 11.1 Hz,  $\text{NCH}_2\text{CH}$ ), 23.49 (C-12) ppm; HRMS (EI)  $m/z$ :  $[\text{M} + \text{Na}]^+$  calcd for  $\text{C}_{26}\text{H}_{24}\text{FN}_3\text{NaO}_4$  484.1643, found 484.1638.

**Compound epi-18.** To a solution of **18** (24.1 mg, 52.3  $\mu\text{mol}$ ) in DMF (100  $\mu\text{L}$ ) was added an aqueous solution of saturated  $\text{K}_2\text{CO}_3$  (20  $\mu\text{L}$ ). The reaction mixture was heated to 130 °C for 10 min, then cooled to rt, diluted with DCM (20 mL), and co-evaporated to a dark orange sludge. The crude product was purified *via* flash chromatography (1:1 hexanes/EtOAc) to yield **epi-18** a light yellow solid (22.6 mg, 49.0  $\mu\text{mol}$ , 94% yield).  $R_f$  (2:8 hexanes/EtOAc) = 0.53;  $^1\text{H}$  NMR (400 MHz,  $\text{CDCl}_3$ ):  $\delta$  = 7.85 (s, 3H, NH), 7.54 (d, 1H,  $J$  = 7.63 Hz, H-11), 7.32 (d, 1H,  $J$  = 8.07 Hz, H-8), 7.23 (t, 1H,  $J$  = 7.12 Hz, H-9), 7.17 (t, 1H,  $J$  = 7.10 Hz, H-10), 6.97 (s, 1H, H-6), 6.82 (s, 1H, H-2'), 6.73 (m, 2H, H-5'/6'), 5.95 (s, 2H, H-7'), 5.20 (quin, 1H,  $J$  = 5.60,  $^2J_{\text{H-F}}$  = 55.61 Hz,  $\text{CHF}$ ), 4.37 (dd, 1H,  $J$  = 4.18, 11.81 Hz, H-12a), 4.09 (d, 1H,  $J$  = 17.2 Hz, H-3), 3.96 (m, 1H,  $J$  = 17.2 Hz, H-3), 3.73 (dd, 1H,  $J$  = 8.73, 13.72 Hz,  $\text{NCH}_2\text{CH}$ ), 3.55 (dd, 1H,  $J$  = 4.18, 15.48 Hz, H-12), 3.32 (dd, 1H,  $J$  = 7.70, 13.72 Hz,  $\text{NCH}_2\text{CH}$ ), 2.93 (dd, 1H,  $J$  = 11.80, 15.50 Hz, H-12), 2.63–2.78 (m, 1H,  $\text{NCH}_2\text{CH}$ ), 2.29–2.48 (m, 2H,  $(\text{CH}_2)_2\text{CHF}$ ), 2.12–2.29 (m, 2H,  $(\text{CH}_2)_2\text{CHF}$ ) ppm;  $^{13}\text{C}$  NMR (126 MHz,  $\text{CDCl}_3$ ):  $\delta$  = 165.69 (C=O), 161.56 (C=O), 148.23 ( $\text{C}_{\text{Ar}}$ ), 148.14 ( $\text{C}_{\text{Ar}}$ ), 136.31 ( $\text{C}_{\text{Ar}}$ ), 131.91 ( $\text{C}_{\text{Ar}}$ ), 129.74 ( $\text{C}_{\text{Ar}}$ ), 126.23 ( $\text{C}_{\text{Ar}}$ ), 122.87 ( $\text{CH}_{\text{Ar}}$ ), 122.56 ( $\text{CH}_{\text{Ar}}$ ), 120.20 ( $\text{CH}_{\text{Ar}}$ ), 118.46 ( $\text{CH}_{\text{Ar}}$ ), 111.15 ( $\text{CH}_{\text{Ar}}$ ), 109.20 ( $\text{CH}_{\text{Ar}}$ ), 109.12 ( $\text{C}_{\text{Ar}}$ ), 108.37 ( $\text{CH}_{\text{Ar}}$ ), 101.40 (C-7'), 87.18 (d,  $^1J_{\text{C-F}}$  = 205.9 Hz,  $\text{CHF}$ ), 52.55 and 51.87 (C-6/12a), 50.06, 50.05, and 49.49 (2  $\times$   $\text{NCH}_2\text{CH}$ , C-3), 33.95 (d,  $^2J_{\text{C-F}}$  = 46.9 Hz,  $(\text{CH}_2)_2\text{CHF}$ ), 33.78 (d,  $^2J_{\text{C-F}}$  = 46.9 Hz,  $(\text{CH}_2)_2\text{CHF}$ ), 27.79 (C-12), 25.37 (d,  $^3J_{\text{C-F}}$  = 11.1

H<sub>2</sub>, NCH<sub>2</sub>CH) ppm; HRMS (EI) *m/z*: [M + Na]<sup>+</sup> calcd for C<sub>26</sub>H<sub>24</sub>N<sub>3</sub>NaO<sub>4</sub> 484.1643, found 484.1635.

**Compound 19.** To a solution of chloroacetyl *cis*-tetrahydro- $\beta$ -carboline **14** (120 mg, 0.281 mmol) in DMF (4 mL) were added 3-(aminomethyl)cyclobutanol hydrochloride (46 mg, 0.33 mmol, 1.2 equiv) and *N,N*-diisopropylethylamine (DIPEA) (97  $\mu$ L, 0.56 mmol, 2 equiv). After 24 h stirring at rt, the reaction was diluted with a 10% solution of NH<sub>4</sub>Cl (10 mL) and extracted with 3  $\times$  DCM (10 mL). The organic was dried over Na<sub>2</sub>SO<sub>4</sub> and concentrated to a brown goo, which was purified *via* flash chromatography (1:1  $\rightarrow$  2:8 hexanes/EtOAc) to yield **19** as a white solid (76.6 mg, 0.167 mmol, 59% yield). *R*<sub>f</sub> (EtOAc) = 0.15; <sup>1</sup>H NMR (498 MHz, CDCl<sub>3</sub>):  $\delta$  = 7.97 (br. s, 1H, NH), 7.62 (d, 1H, *J* = 7.33 Hz, H-11), 7.30 (d, 1H, *J* = 7.69 Hz, H-8), 7.13–7.24 (m, 2H, H-9/10), 6.85 (dd, 2H, *J* = 1.19, 7.97 Hz, H-6'), 6.74 (d, 1H, *J* = 1.47 Hz, H-2'), 6.70 (d, 1H, *J* = 8.06 Hz, H-5'), 6.20 (s, 1H, H-6), 5.88 (d, 2H, *J* = 10.26 Hz, H-7), 4.54 (m, 1H, CHOH), 4.32 (dd, 1H, *J* = 4.39, 11.35 Hz, H-12a), 4.07 (d, 1H, *J* = 17.21 Hz, H-3), 3.92 (d, 1H, *J* = 17.40 Hz, H-3), 3.76 (dd, 1H, *J* = 4.80, 16.10 Hz, H-12), 3.74 (dd, 1H, *J* = 8.61, 13.55 Hz, NCH<sub>2</sub>CH), 3.43 (dd, 1H, *J* = 8.06, 13.73 Hz, NCH<sub>2</sub>CH), 3.23 (dd, 1H, *J* = 11.81, 15.66 Hz, H-12), 2.58 (m, 1H, NCH<sub>2</sub>CH), 2.13–2.21 (m, 2H, (CH<sub>2</sub>)<sub>2</sub>CHOH), 2.07–2.13 (m, 2H, (CH<sub>2</sub>)<sub>2</sub>CHOH), 1.90 (br. s., 1H, OH) ppm; <sup>13</sup>C NMR (125 MHz, CDCl<sub>3</sub>):  $\delta$  = 167.11 (C=O), 166.49 (C=O), 147.89 (C<sub>Ar</sub>), 147.17 (C<sub>Ar</sub>), 136.51 (C<sub>Ar</sub>), 135.23 (C<sub>Ar</sub>), 132.76 (C<sub>Ar</sub>), 126.18 (C<sub>Ar</sub>), 122.54 (CH<sub>Ar</sub>), 120.61 (CH<sub>Ar</sub>), 120.14 (CH<sub>Ar</sub>), 118.61 (CH<sub>Ar</sub>), 111.22 (CH<sub>Ar</sub>), 108.27 (CH<sub>Ar</sub>), 107.36 (CH<sub>Ar</sub>), 106.51 (C<sub>Ar</sub>), 101.17 (C-7'), 63.63 (CHOH), 56.41 and 56.17 (C6/12a), 51.75 and 50.90 (NCH<sub>2</sub>CH/C-3), 38.28 ((CH<sub>2</sub>)<sub>2</sub>CHOH), 37.99 ((CH<sub>2</sub>)<sub>2</sub>CHOH), 23.93 (NCH<sub>2</sub>CH), 23.51 (C-12) ppm; HRMS (EI) *m/z*: [M + Na]<sup>+</sup> calcd for C<sub>26</sub>H<sub>25</sub>N<sub>3</sub>NaO<sub>5</sub> 459.1793, found 459.1794.

**Compound 20.** To a solution of **19** (25.5 mg, 55.5  $\mu$ mol) in pyridine (3 mL) was added tosyl chloride (142 mg, 0.745 mmol, 13.5 equiv). After stirring at rt for 24 h, the reaction was diluted with DCM (20 mL) and washed with saturated NaHCO<sub>3</sub> (aq) and H<sub>2</sub>O, and the organic layer dried over Na<sub>2</sub>SO<sub>4</sub>. The organic solvent was removed under *vacuo*, and the residue was purified *via* flash chromatography (3:7  $\rightarrow$  1:9 hexanes/EtOAc) to yield **20** as a white solid (29.0 mg, 47.3  $\mu$ mol, 85% yield). *R*<sub>f</sub> (EtOAc) = 0.41; <sup>1</sup>H NMR (498 MHz, CDCl<sub>3</sub>):  $\delta$  = 8.00 (s, 1H, NH), 7.79 (d, 2H, *J* = 8.24 Hz, OTs), 7.61 (d, 1H, *J* = 7.33 Hz, H-11), 7.36 (d, 2H, *J* = 8.06 Hz, OTs), 7.29 (m, 1H, H-8), 7.14–7.23 (m, 2H, H9/10), 6.82 (dd, 1H, *J* = 1.56, 7.97 Hz, H-6'), 6.71 (d, 1H, *J* = 1.47 Hz, H-2'), 6.68 (d, 1H, *J* = 8.06 Hz, H-5'), 6.18 (s, 1H, H-6), 5.87 (m, 2H, H-7'), 4.97 (quin, 1H, *J* = 6.55 Hz, CHOTs), 4.29 (dd, 1H, *J* = 4.39, 11.54 Hz, H-12a), 4.03 (d, 1H, *J* = 17.21 Hz, H-3), 3.86 (d, 1H, *J* = 17.21 Hz, H-3), 3.73 (dd, 1H, *J* = 4.67, 16.02 Hz, H-12), 3.68 (dd, 1H, *J* = 8.24, 13.92 Hz, NCH<sub>2</sub>CH), 3.37 (dd, 1H, *J* = 7.97, 13.83 Hz, NCH<sub>2</sub>CH), 3.20 (dd, 1H, *J* = 11.90, 15.57 Hz, H-12), 2.62 (s, 1H, NCH<sub>2</sub>CH), 2.47 (s, 3H, PhCH<sub>3</sub>), 2.30–2.40 (m, 2H, (CH<sub>2</sub>)<sub>2</sub>CHO), 2.11–2.20 (m, 2H, (CH<sub>2</sub>)<sub>2</sub>CHO) ppm; <sup>13</sup>C NMR (125 MHz, CDCl<sub>3</sub>):  $\delta$  = 166.83 (C=O), 166.81 (C=O), 147.89 (C<sub>Ar</sub>), 147.18 (C<sub>Ar</sub>), 144.85 (C<sub>Ar</sub>), 136.52 (C<sub>Ar</sub>), 135.12 (C<sub>Ar</sub>), 133.75 (C<sub>Ar</sub>), 132.74 (C<sub>Ar</sub>), 129.90 (CH<sub>Ar</sub>), 127.83 (CH=), 126.14 (C<sub>Ar</sub>), 122.56 (CH<sub>Ar</sub>), 120.65 (CH<sub>Ar</sub>), 120.15 (CH<sub>Ar</sub>), 118.57 (CH<sub>Ar</sub>), 111.24 (CH<sub>Ar</sub>), 108.24 (CH<sub>Ar</sub>), 107.38 (CH<sub>Ar</sub>), 106.39 (C<sub>Ar</sub>), 101.19 (C-7'), 73.89 (CHOTs), 56.47 and 56.13 (C6/12a), 50.38 and 50.05 (NCH<sub>2</sub>CH/C-3), 33.34

((CH<sub>2</sub>)<sub>2</sub>CHOTs), 33.19 ((CH<sub>2</sub>)<sub>2</sub>CHOTs), 26.60 (NCH<sub>2</sub>CH), 23.54 (C-12), 21.66 (CH<sub>3</sub>) ppm; HRMS (EI) *m/z*: [M + Na]<sup>+</sup> calcd for C<sub>33</sub>H<sub>31</sub>N<sub>3</sub>NaO<sub>7</sub>S 636.1775, found 636.1775.

**Compound [<sup>18</sup>F]epi-18. Radiofluorination Method A.** No-carrier-added [<sup>18</sup>F]fluoride in cyclotron water (0.5–1.5 GBq, 1.5 mL) was trapped on an unconditioned Waters Sep-Pak Accell Plus QMA Carbonate (130 mg) cartridge. The cartridge was predried with 10 mL of air, followed by elution of the [<sup>18</sup>F]fluoride with a solution of Kryptofix 2.2.2/K<sub>2</sub>CO<sub>3</sub> (7–10 mg of Kryptofix 2.2.2, 7–10  $\mu$ L of 1 M K<sub>2</sub>CO<sub>3</sub>, 40  $\mu$ L of H<sub>2</sub>O, 900  $\mu$ L of CH<sub>3</sub>CN) into a glass V-vial. The [<sup>18</sup>F]fluoride solution was dried azeotropically at 100 °C under nitrogen flow. Two aliquots of dry CH<sub>3</sub>CN (2  $\times$  1.5 mL) were added to the residual K[<sup>18</sup>F]F·K<sub>222</sub> complex during the drying process. The final dried complex was dissolved in 1 mL of CH<sub>3</sub>CN or DMF to make the [<sup>18</sup>F]fluoride stock solution. To a V-vial containing precursor **20** (1.0 mg, 1.6  $\mu$ mol) was added 200  $\mu$ L of stock [<sup>18</sup>F]fluoride solution, and the <sup>18</sup>F-labeling was performed at 90 °C using an oil bath. To analyze the reaction mixture and determine radiochemical yield, samples were taken and diluted in 600  $\mu$ L of HPLC eluent for radio-HPLC analysis at 10 and 20 min reaction time points. Semipreparative HPLC was performed as described in the [General Radiochemistry Procedures](#) section. [<sup>18</sup>F]epi-18 elutes at ~12.40 min.

**Radiofluorination Method B.** No-carrier-added [<sup>18</sup>F]fluoride in cyclotron water (0.5–1.5 GBq, 1.5 mL) was trapped on a preconditioned (1 mL of EtOH, 5 mL of H<sub>2</sub>O) Chromafix 30 PS-HCO<sub>3</sub><sup>-</sup> (130 mg) cartridge. The cartridge was predried with 10 mL of air, followed by elution of the [<sup>18</sup>F]fluoride with a solution of TBA·HCO<sub>3</sub> (300  $\mu$ L, 0.075 M in H<sub>2</sub>O) in CH<sub>3</sub>CN (300  $\mu$ L) into a glass V-vial or microcentrifuge tube. The [<sup>18</sup>F]fluoride solution was dried azeotropically at 100 °C under nitrogen flow. Two aliquots of dry CH<sub>3</sub>CN (2  $\times$  1.5 mL) were added to the residual [<sup>18</sup>F]fluoride/TBA complex during the drying process. The final dried complex was dissolved in 1 mL of CH<sub>3</sub>CN to make the [<sup>18</sup>F]fluoride stock solution for exploring reaction conditions or 200  $\mu$ L of CH<sub>3</sub>CN for higher-concentrated stock solutions for animal studies. To a V-vial containing precursor **20** (1.0 mg, 1.6  $\mu$ mol) was added 200  $\mu$ L of stock [<sup>18</sup>F]fluoride, and the <sup>18</sup>F-labeling was performed at 90 °C using an oil bath, or an Eppendorf ThermoMixer in the case of the microcentrifuge tube. After 20 min, the reaction was diluted with 600  $\mu$ L of HPLC eluent (60% CH<sub>3</sub>CN) and injected onto HPLC, using the same HPLC conditions as described in the [General Radiochemistry Procedures](#) section. The fraction collected between ca. 11.8–12.7 min was diluted in 15 mL of H<sub>2</sub>O and passed through a C18 Sep Pak Light cartridge, and then the cartridge was washed with 10 mL of H<sub>2</sub>O. [<sup>18</sup>F]epi-18 was eluted from the cartridge with 0.5 mL of EtOH, and the final solution volume was reduced to 15  $\mu$ L by heating to 90 °C under a stream of nitrogen. The ethanol solution was diluted in 0.9% saline (500  $\mu$ L) and sterile-filtered. Radiochemical purity was confirmed by a final quality control radio-HPLC run.

**Radiofluorination Method C.** No-carrier-added [<sup>18</sup>F]fluoride in cyclotron water (1.0–1.5 GBq, 1.5 mL) was trapped on a preconditioned (10 mL H<sub>2</sub>O) Waters Sep-Pak Accell Plus Light QMA Carbonate (46 mg) cartridge. The cartridge was predried with 10 mL of air, followed by elution of the [<sup>18</sup>F]fluoride with a solution of TFA in H<sub>2</sub>O/CH<sub>3</sub>CN (18

$\mu\text{L}$  of TFA, 100  $\mu\text{L}$  of  $\text{H}_2\text{O}$ , 400  $\mu\text{L}$  of  $\text{CH}_3\text{CN}$ ) into a glass V-vial containing  $\text{Fe}(\text{acac})_3$  (15.0 mg, 42.5  $\mu\text{mol}$ ). The elution efficiency of [ $^{18}\text{F}$ ]fluoride off the QMA averages  $\sim 80\%$ . The V-vial was sealed, and the [ $^{18}\text{F}$ ]fluoride solution was heated at 80  $^\circ\text{C}$  for 10 min. The vial was then opened and heated to 110  $^\circ\text{C}$  for 15 min until dryness, resulting in a loss of  $\sim 20\%$  activity. A solution of precursor **20** (1.0 mg, 1.6  $\mu\text{mol}$ ) in dry 1,4-dioxane (50  $\mu\text{L}$ ) was added to the V-vial; then, the vial was sealed and heated at 120  $^\circ\text{C}$  for 20 min. The reaction was removed from heat and allowed to cool for a few minutes, then diluted with 500  $\mu\text{L}$  of HPLC eluent (60%  $\text{CH}_3\text{CN}$ ), and filtered through a 0.22  $\mu\text{m}$  filter (Millipore Millex-GV PVDF). The filtered solution was injected onto HPLC, using the same HPLC conditions as described in the General Radiochemistry Procedures section.

## ■ ASSOCIATED CONTENT

### SI Supporting Information

The Supporting Information is available free of charge at <https://pubs.acs.org/doi/10.1021/acsomega.1c03315>.

NMR characterization of all compounds; HPLC UV and radio-chromatograms for  $^{18}\text{F}$ -labeling of precursor **20** with [ $^{18}\text{F}$ ]TBAF/TBA· $\text{HCO}_3$  (Figure S1) and epimerization of precursor **20** in  $\text{CH}_3\text{CN}$  (Table S1) (PDF)

## ■ AUTHOR INFORMATION

### Corresponding Author

Justin J. Bailey – Department of Oncology, Cross Cancer Institute, University of Alberta, Edmonton, Alberta T6G 1Z2, Canada; [orcid.org/0000-0002-8280-5712](https://orcid.org/0000-0002-8280-5712); Phone: +1-780-988-4622; Email: [jjbailey@ualberta.ca](mailto:jjbailey@ualberta.ca); Fax: +1-780-492-7303

### Authors

Melinda Wuest – Department of Oncology, Cross Cancer Institute, University of Alberta, Edmonton, Alberta T6G 1Z2, Canada

Tamara Bojovic – Department of Oncology, Cross Cancer Institute, University of Alberta, Edmonton, Alberta T6G 1Z2, Canada

Travis Kronemann – Department of Oncology, Cross Cancer Institute, University of Alberta, Edmonton, Alberta T6G 1Z2, Canada

Carmen Wängler – Biomedical Chemistry, Department of Clinical Radiology and Nuclear Medicine, Medical Faculty Mannheim of Heidelberg University, Mannheim 68167, Germany

Björn Wängler – Molecular Imaging and Radiochemistry, Department of Clinical Radiology and Nuclear Medicine, Medical Faculty Mannheim of Heidelberg University, Mannheim 68167, Germany

Frank Wuest – Department of Oncology, Cross Cancer Institute, University of Alberta, Edmonton, Alberta T6G 1Z2, Canada; [orcid.org/0000-0002-6705-6450](https://orcid.org/0000-0002-6705-6450)

Ralf Schirmacher – Department of Oncology, Cross Cancer Institute, University of Alberta, Edmonton, Alberta T6G 1Z2, Canada; [orcid.org/0000-0002-7098-3036](https://orcid.org/0000-0002-7098-3036)

Complete contact information is available at:

<https://pubs.acs.org/doi/10.1021/acsomega.1c03315>

## Author Contributions

This manuscript was written through contributions of all authors.

## Funding

This work was financially supported by the Natural Sciences and Engineering Research Council (NSERC) to R.S.

## Notes

The authors declare no competing financial interest.

## ■ ACKNOWLEDGMENTS

The authors thank Dr. Esther Schirmacher for reading the manuscript and providing useful feedback. They also thank Angelina Morales-Izquierdo for the mass spectrometry analysis.

## ■ ABBREVIATIONS

AD	Alzheimer's disease
$A_m$	molar activity
$B_{\text{max}}$	total density of receptors
BBB	blood–brain barrier
cAMP	cyclic adenosine 3',5'-monophosphate
cGMP	cyclic guanosine 3',5'-monophosphate
$\text{CH}_3\text{CN}$	acetonitrile
CIAT	crystallization-induced asymmetric transformation
DMF	dimethylformamide
ED	erectile dysfunction
$K_{222}$	Kryptofix 222
$\text{K}_2\text{CO}_3$	potassium carbonate
MIP	maximum-intensity projections
nosylate	4-nitrobenzenesulfonate
PDE	phosphodiesterase
PET	positron emission tomography
QC	quality control
RCC	radiochemical conversion
TAC	time–activity curves
$\text{TBA}\cdot\text{HCO}_3$	tetrabutylammonium bicarbonate
tosylate	methylbenzenesulfonate
triflate	trifluoromethanesulfonate

## ■ REFERENCES

- (1) Fajardo, A. M.; Piazza, G. A.; Tinsley, H. N. The Role of Cyclic Nucleotide Signaling Pathways in Cancer: Targets for Prevention and Treatment. *Cancers* **2014**, *6*, 436–458.
- (2) Ahmad, F.; Murata, T.; Simizu, K.; Degerman, E.; Maurice, D.; Manganiello, V. Cyclic Nucleotide Phosphodiesterases: important signaling modulators and therapeutic targets. *Oral Dis.* **2015**, *21*, e25–e50.
- (3) Francis, S. H.; Blount, M. A.; Corbin, J. D. Mammalian Cyclic Nucleotide Phosphodiesterases: Molecular Mechanisms and Physiological Functions. *Physiol. Rev.* **2011**, *91*, 651–690.
- (4) Maurice, D. H.; Ke, H.; Ahmad, F.; Wang, Y.; Chung, J.; Manganiello, V. C. Advances in targeting cyclic nucleotide phosphodiesterases. *Nat. Rev. Drug Discovery* **2014**, *13*, 290–314.
- (5) Drilon, A.; Nagasubramanian, R.; Blake, J. F.; Ku, N.; Tuch, B. B.; Ebata, K.; Smith, S.; Lauriault, V.; Kolakowski, G. R.; Brandhuber, B. J.; Larsen, P. D.; Bouhana, K. S.; Winski, S. L.; Hamor, R.; Wu, W.-L.; Parker, A.; Morales, T. H.; Sullivan, F. X.; DeWolf, W. E.; Wollenberg, L. A.; Gordon, P. R.; Douglas-Lindsay, D. N.; Scaltriti, M.; Benayed, R.; Raj, S.; Hanusch, B.; Schram, A. M.; Jonsson, P.; Berger, M. F.; Hechtman, J. F.; Taylor, B. S.; Andrews, S.; Rothenberg, S. M.; Hyman, D. M. A Next-Generation TRK Kinase Inhibitor Overcomes Acquired Resistance to Prior TRK Kinase Inhibition in Patients with TRK Fusion-Positive Solid Tumors. *Cancer Discovery* **2017**, *7*, 963–972.

- (6) Terrett, N. K.; Bell, A. S.; Brown, D.; Ellis, P. Sildenafil (VIAGRA), a potent and selective inhibitor of type 5 cGMP phosphodiesterase with utility for the treatment of male erectile dysfunction. *Bioorg. Med. Chem. Lett.* **1996**, *6*, 1819–1824.
- (7) Galiè, N.; Ghofrani, H. A.; Torbicki, A.; Barst, R. J.; Rubin, L. J.; Badesch, D.; Fleming, T.; Parpia, T.; Burgess, G.; Branzi, A.; Grimminger, F.; Kurzyna, M.; Simonneau, G. Sildenafil Citrate Therapy for Pulmonary Arterial Hypertension. *N. Engl. J. Med.* **2005**, *353*, 2148–2157.
- (8) Roehrborn, C. G.; Kaminetsky, J. C.; Auerbach, S. M.; Montelongo, R. M.; Elion-Mboussa, A.; Viktrup, L. Changes in peak urinary flow and voiding efficiency in men with signs and symptoms of benign prostatic hyperplasia during once daily tadalafil treatment. *BJU Int.* **2010**, *105*, 502–507.
- (9) Lin, C. S. Tissue expression, distribution, and regulation of PDE5. *Int. J. Impotence Res.* **2004**, *16*, S8–S10.
- (10) Zhang, W.-H.; Zhang, X.-H. Clinical and preclinical treatment of urologic diseases with phosphodiesterase isoenzymes 5 inhibitors: an update. *Asian J. Androl.* **2016**, *18*, 723–731.
- (11) Barone, I.; Giordano, C.; Bonofiglio, D.; Andò, S.; Catalano, S. Phosphodiesterase type 5 and cancers: progress and challenges. *Oncotarget* **2017**, *8*, 99179–99202.
- (12) Peng, T.; Gong, J.; Jin, Y.; Zhou, Y.; Tong, R.; Wei, X.; Bai, L.; Shi, J. Inhibitors of phosphodiesterase as cancer therapeutics. *Eur. J. Med. Chem.* **2018**, *150*, 742–756.
- (13) Catalano, S.; Panza, S.; Augimeri, G.; Giordano, C.; Malivindi, R.; Gelsomino, L.; Marsico, S.; Giordano, F.; Györfy, B.; Bonofiglio, D.; Andò, S.; Barone, I. Phosphodiesterase 5 (PDE5) Is Highly Expressed in Cancer-Associated Fibroblasts and Enhances Breast Tumor Progression. *Cancers* **2019**, *11*, No. 1740.
- (14) Pantziarka, P.; Sukhatme, V.; Crispino, S.; Bouche, G.; Meheus, L.; Sukhatme, V. P. Repurposing drugs in oncology (ReDO)-selective PDE5 inhibitors as anti-cancer agents. *Ecancermedicalscience* **2018**, *12*, 824.
- (15) Teich, A. F.; Sakurai, M.; Patel, M.; Holman, C.; Saeed, F.; Fiorito, J.; Arancio, O. PDE5 Exists in Human Neurons and is a Viable Therapeutic Target for Neurologic Disease. *J. Alzheimers Dis.* **2016**, *52*, 295–302.
- (16) Mostafa, T. Could Oral Phosphodiesterase 5 Inhibitors Have a Potential Adjuvant Role in Combating COVID-19 Infection? *Sex Med. Rev.* **2021**, *9*, 15–22.
- (17) Isidori, A. M.; Giannetta, E.; Pofi, R.; Venneri, M. A.; Gianfrilli, D.; Campolo, F.; Mastroianni, C. M.; Lenzi, A.; d’Ettorre, G. Targeting the NO-cGMP-PDE5 pathway in COVID-19 infection. The DEDALO project. *Andrology* **2021**, *9*, 33–38.
- (18) Shirvalilo, M. Targeting the SARS-CoV-2 3CLpro and NO/cGMP/PDE5 pathway in COVID-19: a commentary on PDE5 inhibitors. *Future Cardiol.* **2021**, DOI: 10.2217/fca-2020-0201.
- (19) Jakobsen, S.; Kodahl, G. M.; Olsen, A. K.; Cumming, P. Synthesis, radiolabeling and in vivo evaluation of [<sup>11</sup>C]RAL-01, a potential phosphodiesterase 5 radioligand. *Nucl. Med. Biol.* **2006**, *33*, 593–597.
- (20) Chekol, R.; Gheysens, O.; Cleynhens, J.; Pokreisz, P.; Vanhoof, G.; Ahamed, M.; Janssens, S.; Verbruggen, A.; Bormans, G. Evaluation of PET radioligands for in vivo visualization of phosphodiesterase 5 (PDE5). *Nucl. Med. Biol.* **2014**, *41*, 155–162.
- (21) Gómez-Vallejo, V.; Ugarte, A.; García-Barroso, C.; Cuadrado-Tejedor, M.; Szczupak, B.; Dopeso-Reyes, I. G.; Lanciego, J. L.; García-Osta, A.; Llop, J.; Oyarzabal, J.; Franco, R. Pharmacokinetic investigation of sildenafil using positron emission tomography and determination of its effect on cerebrospinal fluid cGMP levels. *J. Neurochem.* **2016**, *136*, 403–415.
- (22) Cumming, P. A business of some heat: molecular imaging of phosphodiesterase 5. *J. Neurochem.* **2016**, *136*, 220–221.
- (23) Liu, J.; Wenzel, B.; Dukic-Stefanovic, S.; Teodoro, R.; Ludwig, F.-A.; Deuther-Conrad, W.; Schröder, S.; Chezal, J.-M.; Moreau, E.; Brust, P.; Maisson-Besset, A. Development of a New Radio-fluorinated Quinoline Analog for PET Imaging of Phosphodiesterase 5 (PDE5) in Brain. *Pharmaceuticals* **2016**, *9*, No. 22.
- (24) Fiorito, J.; Saeed, F.; Zhang, H.; Staniszewski, A.; Feng, Y.; Francis, Y. L.; Rao, S.; Thakkar, D. M.; Deng, S.-X.; Landry, D. W.; Arancio, O. Synthesis of quinoline derivatives: Discovery of a potent and selective phosphodiesterase 5 inhibitor for the treatment of Alzheimer’s disease. *Eur. J. Med. Chem.* **2013**, *60*, 285–294.
- (25) Wenzel, B.; Liu, J.; Dukic-Stefanovic, S.; Deuther-Conrad, W.; Teodoro, R.; Ludwig, F.-A.; Chezal, J.-M.; Moreau, E.; Brust, P.; Maisson-Besset, A. Targeting cyclic nucleotide phosphodiesterase 5 (PDE5) in brain: Toward the development of a PET radioligand labeled with fluorine-18. *Bioorg. Chem.* **2019**, *86*, 346–362.
- (26) Chekol, R.; Gheysens, O.; Ahamed, M.; Cleynhens, J.; Pokreisz, P.; Vanhoof, G.; Janssens, S.; Verbruggen, A.; Bormans, G. Carbon-11 and Fluorine-18 Radiolabeled Pyridopyrazinone Derivatives for Positron Emission Tomography (PET) Imaging of Phosphodiesterase-5 (PDE5). *J. Med. Chem.* **2017**, *60*, 486–496.
- (27) Dong, F.; Du, J.; Miao, C.; Jia, L.; Li, W.; Wang, M.; Zheng, Q.-H.; Xu, Z. Radiosynthesis of carbon-11 labeled PDE5 inhibitors as new potential PET radiotracers for imaging of Alzheimer’s disease. *Appl. Radiat. Isot.* **2019**, *154*, No. 108873.
- (28) Xu, Z.; Jia, L.; Liu, W.; Li, W.; Song, Y.; Zheng, Q.-H. Radiosynthesis of a carbon-11 labeled PDE5 inhibitor [<sup>11</sup>C]TPN171 as a new potential PET heart imaging agent. *Appl. Radiat. Isot.* **2020**, *162*, No. 109190.
- (29) Ugarte, A.; Gil-Bea, F.; García-Barroso, C.; Cedazo-Minguez, A.; Ramírez, M. J.; Franco, R.; García-Osta, A.; Oyarzabal, J.; Cuadrado-Tejedor, M. Decreased levels of guanosine 3’, 5’-monophosphate (cGMP) in cerebrospinal fluid (CSF) are associated with cognitive decline and amyloid pathology in Alzheimer’s disease. *Neuropathol. Appl. Neurobiol.* **2015**, *41*, 471–482.
- (30) Corbin, J. D.; Beasley, A.; Blount, M. A.; Francis, S. H. High lung PDE5: A strong basis for treating pulmonary hypertension with PDE5 inhibitors. *Biochem. Biophys. Res. Commun.* **2005**, *334*, 930–938.
- (31) Maw, G. N.; Allerton, C. M. N.; Gbekor, E.; Million, W. A. Design, synthesis and biological activity of  $\beta$ -carboline-based type-5 phosphodiesterase inhibitors. *Bioorg. Med. Chem. Lett.* **2003**, *13*, 1425–1428.
- (32) Beghyn, T.; Hounsou, C.; Deprez, B. P. PDE5 inhibitors: An original access to novel potent arylated analogues of tadalafil. *Bioorg. Med. Chem. Lett.* **2007**, *17*, 789–792.
- (33) Kuchar, M.; Mamat, C. Methods to Increase the Metabolic Stability of <sup>18</sup>F-Radiotracers. *Molecules* **2015**, *20*, 16186–16220.
- (34) Shoup, T. M.; Goodman, M. M. Synthesis of [F-18]-1-amino-3-fluorocyclobutane-1-carboxylic acid (FACBC): a PET tracer for tumor delineation. *J. Labelled Compd. Radiopharm.* **1999**, *42*, 215–225.
- (35) Franck, D.; Kniess, T.; Steinbach, J.; Zitzmann-Kolbe, S.; Friebe, M.; Dinkelborg, L. M.; Graham, K. Investigations into the synthesis, radiofluorination and conjugation of a new [18F]-fluorocyclobutyl prosthetic group and its in vitro stability using a tyrosine model system. *Bioorg. Med. Chem.* **2013**, *21*, 643–652.
- (36) Daugan, A.; Grondin, P.; Ruault, C.; Le Monnier de Gouville, A.-C.; Coste, H.; Kirilovsky, J.; Hyafil, F.; Labaudinière, R. The Discovery of Tadalafil: A Novel and Highly Selective PDE5 Inhibitor. 1: 5,6,11,11a-Tetrahydro-1H-imidazo[1’,5’:1,6]pyrido[3,4-b]indole-1,3(2H)-dione Analogues. *J. Med. Chem.* **2003**, *46*, 4525–4532.
- (37) Daugan, A.; Grondin, P.; Ruault, C.; Le Monnier de Gouville, A.-C.; Coste, H.; Linget, J. M.; Kirilovsky, J.; Hyafil, F.; Labaudinière, R. The Discovery of Tadalafil: A Novel and Highly Selective PDE5 Inhibitor. 2: 2,3,6,7,12,12a-hexahydropyrazino[1’,2’:1,6]pyrido[3,4-b]indole-1,4-dione Analogues. *J. Med. Chem.* **2003**, *46*, 4533–4542.
- (38) Shi, X.-X.; Liu, S.-L.; Xu, W.; Xu, Y.-L. Highly stereoselective Pictet–Spengler reaction of d-tryptophan methyl ester with piperonal: convenient syntheses of Cialis (Tadalafil), 12a-epi-Cialis, and their deuterated analogues. *Tetrahedron: Asymmetry* **2008**, *19*, 435–442.
- (39) Ahmed, N. S.; Ali, A. H.; El-Nashar, S. M.; Gary, B. D.; Fajardo, A. M.; Tinsley, H. N.; Piazza, G. A.; Negri, M.; Abadi, A. H. Exploring the PDE5 H-pocket by ensemble docking and structure-based design

and synthesis of novel  $\beta$ -carboline derivatives. *Eur. J. Med. Chem.* **2012**, *57*, 329–343.

(40) Abadi, A. H.; Gary, B. D.; Tinsley, H. N.; Piazza, G. A.; Abdel-Halim, M. Synthesis, molecular modeling and biological evaluation of novel tadalafil analogues as phosphodiesterase 5 and colon tumor cell growth inhibitors, new stereochemical perspective. *Eur. J. Med. Chem.* **2010**, *45*, 1278–1286.

(41) Gao, W.; Zhang, Z.; Li, Z.; Liang, G. Chiral separation of two pairs of enantiomers of tadalafil by high-performance liquid chromatography. *J. Chromatogr. Sci.* **2007**, *45*, 540–543.

(42) Seok Moon, B.; Hyung Park, J.; Jin Lee, H.; Sun Kim, J.; Sup Kil, H.; Se Lee, B.; Yoon Chi, D.; Chul Lee, B.; Kyeong Kim, Y.; Eun Kim, S. Highly efficient production of [ $^{18}\text{F}$ ]fallypride using small amounts of base concentration. *Appl. Radiat. Isot.* **2010**, *68*, 2279–2284.

(43) Winton, W.; Brooks, A.; Verhoog, S.; Sanford, M.; Scott, P. Nucleophilic Substitution of Secondary Tosylates Utilizing [ $^{18}\text{F}$ ]HF and Iron(III) Acetylacetonate. *J. Nucl. Med.* **2019**, *60*, 1620.

(44) Borthwick, A. D. 2,5-Diketopiperazines: Synthesis, Reactions, Medicinal Chemistry, and Bioactive Natural Products. *Chem. Rev.* **2012**, *112*, 3641–3716.

(45) Corbeil, C. R.; Moitessier, N. Docking Ligands into Flexible and Solvated Macromolecules. 3. Impact of Input Ligand Conformation, Protein Flexibility, and Water Molecules on the Accuracy of Docking Programs. *J. Chem. Inf. Model.* **2009**, *49*, 997–1009.

(46) Zhang, Y.; He, Q.; Ding, H.; Wu, X.; Xie, Y. Improved Synthesis of Tadalafil. *Org. Prep. Proced. Int.* **2005**, *37*, 99–102.